Effect of feed supplementation with docosahexaenoic acid in regio- and enantiopure triacylglycerols on gut metabolome and microbiota in rats

Kang Chen†, Xuetao Wei‡, Zhang Jian§, Haraldur G. Gudmundsson[#], Gudmundur G. Haraldsson[#], Qinghai Sheng[&], Yumei Zhang§*, Baoru Yang†*

†Food Sciences, Department of Life Technologies, University of Turku, FI-20014 Turun yliopisto, Finland

‡Beijing Key Laboratory of Toxicological Research and Risk Assessment for Food Safety, Department of Toxicology, School of Public Health, Beijing University, Beijing 100191, China

§Department of Nutrition and Food Hygiene, School of Public Health, Beijing University, Beijing 100191, China

[#] Science Institute, University of Iceland, IS-107 Reykjavik, Iceland

[&]College of Food Science and Technology, Hebei Agricultural University, Baoding 071001, China

* Author for Correspondence:

Professor Baoru Yang,

baoru.yang@utu.fi; Tel: +358 452737988

*Co-correspondence:

Professor Yumei Zhang

Email: zhangyumei@bjmu.edu.cn; Tel: +8613426134251

Abstract

Docosahexaenoic acid [22:6(n-3), DHA] plays an important role in human physiology including gut health. This research aimed to investigate the impact of positional distribution of DHA in dietary triacylglycerols (TAG) on gut metabolomic profile and microbiota. In the 4-week feeding trial, the Sprague-Dawley rats were fed on an n-3 deficient feed supplemented with TAG containing DHA at the *sn*-1, 2, or 3 position and palmitic acid at the remaining positions. Three groups receiving standard n-3 adequate feed, n-3 deficient feed, or n-3 deficient feed supplemented with tripalmitin were included as controls. The gut metabolome was studied using LC–MS-based non-targeted metabolomics, and microbiota profiles were investigated by 16S rRNA sequencing. Compared to the n-3 adequate diet, four-week feeding on the n-3 deficient diet affected the fecal pyrimidine metabolism, steroid biosynthesis, and arginine and proline metabolism. Feeding with DHA-containing TAGs, especially TAG with DHA at *sn*-3 position, increased the level of N5-Carboxy aminoimidazole ribonucleotide related to purine biosynthesis and dimethylbenzimidazole involved in vitamin B2 biosynthesis. N-3 deficient diet lowered the abundance of the genus *Alistipes* and the species *Bacteroides massiliensis* in the gut microbiota. Compared to the n-3 deficient groups, feeding with DHA-containing TAGs decreased the abundance of species *Prevotella* sp. CAG: 1031, and feeding with *sn*-2 DHA resulted in an increase in the abundance of *Bacteroides fragilis* and a decrease in the abundance of *Faecalibacterium* sp. CAP 74. This is the first study showing that dietary DHA from different positions of TAG may affect gut metabolites and microbiota differently.

Keywords

Docosahexaenoic acid, N-3 deficiency, Positional isomer, Triacylglycerols, Gut microbiota, Gut metabolome

1. Introduction

Triacylglycerols (TAGs) are the main source of fatty acids (FAs) in human diet, including long-chain (n-3) polyunsaturated FAs (n-3 PUFAs) such as docosahexaenoic acid (DHA). DHA takes part in numerous biological functions such as retinal and neural development and prevention of cardiac and circulatory disorders (Hull, 2011; Swanson et al., 2012).

Structures of TAG molecules play an important role not only in the absorption but also the metabolism of dietary n-3 PUFAs. In a TAG molecule, FAs are esterified to three stereospecific positions on the glycerol backbone. The positions occupied by these FAs are numbered relative to their stereospecific numbering (*sn*) as *sn*-1, *sn*-2, and *sn*-3. TAGs are to a large extent chiral in nature (Gunstone & Harwood, 2007) and they are metabolized in the chiral physiological environment (Carrière et al., 1997; Lehner & Kuksis, 1993; Yang et al., 1995, 2011). During digestion, dietary TAGs are hydrolyzed by the action of lipases including gastric lipase and pancreatic lipase, which are normally regio- and enantioselective. For example, gastric lipase of seals has been shown not to hydrolyze long chain n-3 PUFAs at the *sn*-2 position of TAGs (Iverson et al., 1992). Gastric lipases have been reported to hydrolyze FAs at *sn*-3 position faster than those at *sn*-1 position (Duan, 2000). Dog pancreatic lipase has shown preference for n-3 PUFAs at the *sn*-3 position of TAGs (Carrière et al., 1997). Lipoprotein lipase, which hydrolyzes TAGs from chylomicron, has been reported to have positional priority towards the *sn*-1 position (Morley & Kuksis, 1972). We have previously assessed the bioavailability of DHA from enantiopure triacylglycerols and their regioisomeric counterparts in rats, quantitative lipid analysis showed that less fecal excretion of DHA was detected in rats fed with TAGs containing DHA at the *sn*-2 position compared to those fed with DHA at the *sn*-1 or *sn*-3 position of TAGs (Linderborg et al., 2019).

Gut metabolic and microbiota profiles are important for maintaining gut health. DHA supplementation has been revealed to have a regulatory effect on fecal metabolic and microbiota profiles and gut health (Dong et al., 2022; Zhuang et al., 2021). For example, the DHA supplement in the form of algae oil has been reported to alter fecal cholesterol metabolism and purine metabolism pathways and decrease the abundance of *Bacteroides* and *Prevotella_9* in HIV-infected patients (R. Dong et al., 2022). A review has pointed out that DHA supplementation has often accompanied a decrease in *Faecalibacterium* abundance and an increase in *Lachnospiraceae* abundance (Costantini et al., 2017). Supplementation with mixture of EPA and DHA at an equal ratio has been shown to ameliorate the dysfunction of the intestinal barrier and decrease the high PPAR-γ level caused by ischemia and reperfusion intestinal injury in rats (Wang et al., 2012). Studies in both humans and animals emphasize the capacity of omega-3 PUFAs to impact the gut-brain connection by altering the composition of the gut microbiota (Costantini et al., 2017). In addition, supplementation of DHA affected locomotor activity and anxiety-related behaviors of rats with brain diseases (Arteaga et al., 2017; Xiao et al., 2022) and exposed to social isolation stress (Oshima et al., 2017). Enhanced permeability leads to an inflammatory reaction, wherein microglia and peripheral monocytes are activated to traverse the blood-brain barrier, resulting in the release of inflammatory cytokines and neurotoxic molecules, subsequently initiating neuroinflammation. DHA significantly enhances gut barrier integrity by modulating the growth of butyrate-producing bacteria (La Rosa et al., 2018), thus indicating the link of dietary intake of DHA with the brain-gut-microbiota axis. However, little is currently known about how the different regio- and enantiospecific forms of TAGs containing DHA affect the fecal metabolic profile, microbiota composition and locomotor activity. This gap in knowledge has been caused by the challenge in the synthesis of regio- and enantiospecifically structured TAGs in quantities

93 required for *in vivo* studies. Due to the difference in digestion and absorption of enantiospecifically
94 structured TAGs containing DHA, their effect on fecal metabolic profile, microbiota composition
95 and locomotor activity might be also different.

96 The study aimed to investigate i) how n-3 PUFA adequate diet and n-3 PUFA deficient diet
97 affect fecal metabolic profile and microbiota composition; ii) how dietary TAGs possessing DHA
98 either in *sn*-1, *sn*-2 or *sn*-3 position and two palmitic acid residues in the remaining *sn*-positions,
99 [*sn*-22:6(n-3)-16:0-16:0, *sn*-16:0- 22:6(n-3)-16:0 or *sn*-16:0-16:0-22:6(n-3)], supplemented to the
100 n-3 deficient diet, would affect fecal metabolic profile and microbiota composition. To the best of
101 our knowledge, this is the first study comparing the effect of DHA from the *sn*-1, *sn*-2 or *sn*-3
102 positions of TAGs on fecal metabolic profile and microbiota composition. A group fed with n-3
103 deficient diet supplemented tripalmitin was also included to study the impact of increased dietary
104 intake of palmitic acid on gut microbiota.

105 **2. Method and Material**

106 **2.1 Synthesis of regio- and enantiopure structured triacylglycerols**

107 The study was enabled by chemoenzymatic synthesis of regio- and enantiospecific TAGs
108 containing DHA at *sn*-1, 2, or 3 position and palmitic acid in the remaining positions in quantities
109 sufficient for rat feeding and by the development of a powerful method of chiral liquid
110 chromatographic analysis (Kalpio et al., 2020; Kristinsson et al., 2014).

111 **2.2 Animals and diets**

112 The study was approved by the Ethical Committee of Peking University (Ethical approval number:
113 LA202129). Seventy-two male Sprague-Dawley rats (age 21 ± 2 days) were maintained in a
114 specific pathogen-free environment at the Animal Housing Unit of Peking University under
115 controlled temperature (23−25 °C) and a 12 h light/12 h dark cycle. Each rat was housed in one

cage and kept on adaptive feeding of standard AIN-93G diet containing soybean oil as a source of n-3 PUFA for the purpose of adaptation. The composition of AIN-93G diet (Nuoyuan biotechnology Co., Ltd, Beijing, China) is shown in Table S1. After the 7 days of adaptation, the rats were randomly divided into 6 experimental groups, 12 rats in each group, fed with different diet for 4 weeks. Five groups were fed with n-3 deficient AIN-93G feed containing peanut oil (n-3 deficient oil) as the only source of FAs, while the sixth group was on the standard AIN-93G containing soybean oil (n-3 adequate oil, containing precursor n-3 fatty acids but no DHA) as a source of FAs (Con group). The FAs compositions of peanut oil and soybean oil are listed in Table S2. Among the five groups fed with the n-3 deficient feed, four groups received 2,3-dipalmitoyl-1-docosahexaenoyl-*sn*-glycerol (sn1DHA group), 1,3-dipalmitoyl-2-docosahexaenoyl-*sn*-glycerol (sn2DHA group), 1,2-dipalmitoyl-3-docosahexaenoyl-*sn*-glycerol (sn3DHA group), or tripalmitin (Trip group) as the experimental fat at a daily dosage of 500 mg/kg body weight for four weeks, while the fifth group received no fat supplementation serving as the n-3 deficient control (n3De group). The TAG having *sn*-2 DHA is a regioisomer of the TAGs with DHA at *sn*-1 or *sn*-3 position, whereas the latter two TAGs are two enantiomers differing only in the positioning of fatty acids between the two outer positions (*sn*-1 and *sn*-3). The daily dosage of experimental fat was selected based on previous studies on n-3 PUFA interventions (Ghasemifard et al., 2014; Kaur et al., 2010). α-Tocopherol (100 mg/100 g) as an antioxidant was added to the experimental fats before dividing the fat into individual doses. Individual doses were stored under nitrogen at −80 °C. Each daily dosage of experimental fat was embedded in a pellet of n-3 deficient feed. The aliquots of experimental fat were melted quickly using a water bath at 40 °C and pipetted between two halves of feed pellets. The pellets containing the experimental fats were prepared the day before the feeding, stored at dark +4 °C overnight and given to the rats as the first feed in the morning. Rodent

chows are removed from cages during administration of TAGs. Once the experimental fat pellets were consumed completely, the rats were then provided feed *ad libitum*. The n3De and Con groups were provided feed *ad libitum*. The fecal samples were collected on the day 28 and stored for a maximum of 4 weeks before analysis.

2.3 Open field test

The open field test (OFT) is a widely used behavioral assay in rodent research to assess general locomotor activity and anxiety-related behaviors. At the end of the feeding period (the day before sacrifice), all rats were assessed for the general locomotor and exploratory behavior in the open field test (OFT). The 100 × 100 × 50 cm^3 apparatus was constructed and overlaid on an 8 × 8 grid. During testing, the outer walls of the apparatus were covered with dark poster board to ensure rats could not see beyond the apparatus. Rats were individually tested for a period of 5 min and the video tracking software Anymaze (Stoelting AnyMaze Software, Wood Dale, IL, USA) was used for accurate measurements of locomotion. Experimenters were not present in the room during the testing. The animals were tested in a randomized manner. Performance parameters related to locomotor activity were recorded and calculated including total distance traveled, center distance traveled, peripheral distance traveled, time spent in the center quadrant (4 × 4 center grid), time spent in the periphery (all areas except center quadrant), and the number of entries into each zone. Zone entry was defined as the front paws and shoulders being placed into the area. The field was cleaned by wiping with 70% ethanol between each testing rat.

2.4 Non-targeted Fecal Metabolomics

Fecal nontargeted metabolomics analysis (12 fecal samples per group) was performed, the protocol was followed the previous protocol (H. Wang et al., 2022). Briefly, 300 μL of methanol (Merck KGaA, Darmstadt, Hessen, Germany) containing isotopically-labeled internal standards

(Cambridge Isotope Laboratories, Tewksbury, MA, USA) was mixed with fecal sample (100 μg). The supernatant was collected and filtered after centrifuging at 12000 × *g* for 15 min at 4 ℃. The resultant extracts were analysed using a UHPLC system (Vanquish, Thermo Fisher Scientific, Waltham, MA) with a UPLC BEH Amide column (1.7 μm, 2.1 mm *100 mm, Waters) coupled to TripleTOF 5600 (Q-TOF, AB Sciex，Milford, MA, USA). The mobile phase consisted of 25 mM NH_4OAc and 25 mM NH_4OH in water (Merck KGaA)（pH=9.75）(A) and acetonitrile (Merck KGaA) (B) was carried with elution gradient as follows: 0 min, 95% B; 7 min, 65% B; 9 min, 40% B; 9.1 min, 95% B; 12 min, 95% B, which was delivered at 0.5 mL/min. The injection volume was 3 μL. The Triple TOF mass spectrometer was used for its ability to acquire MS/MS spectra on an information-dependent basis (IDA) during an LC/MS experiment. In this mode, the acquisition software (Analyst TF 1.7, AB Sciex) continuously evaluates the full scan survey MS data as it collects and triggers the acquisition of MS/MS spectra depending on preselected criteria. In each cycle, 12 precursor ions whose intensity greater than 100 were chosen for fragmentation at collision energy (CE) of 30 V (15 MS/MS events with product ion accumulation time of 50 msec each). ESI source conditions were set as following: Ion source gas 1 as 60 Psi, Ion source gas 2 as 60 Psi, Curtain gas as 35 Psi, source temperature 650 °C, Ion Spray Voltage Floating 5000 V or –4000 V in positive or negative modes, respectively. Metabolite annotation was carried out by using an in-house MS2 database. MS1 accurate mass tolerance is 0.01 Da. MS2 accurate mass tolerance is 0.05 Da. The normalized peak intensities of the features were used for comparison between different groups. The method of data normalization adopted was total peak area normalization.

2.5 Gut Microbiota Analysis

The genomic DNA extraction from feces, PCR amplification, and sequencing (n = 6, each group) were conducted by following the protocol described previously (X. Dong et al., 2022). Briefly, the

total bacterial DNA was extracted from the colonic content by using a TIANamp Stool DNA kit (TIANGEN Bio-Tech Co., Ltd, Beijing, China). The V4 region of the 16S rRNA gene was amplified using specific primers with the barcode (515F: GTGCCAGCMGCCGCGGTAA and 806R: GGACTACHVGGGTWTCTAAT). After amplification of V4 hypervariable region of the bacterial 16S rRNA gene, the resulting PCR products were extracted, purified, and quantified. DNA library was constructed using the TruSeq DNA Sample Prep kit (Illumina, San Diego, CA, USA) and sequenced on an Illumina MiSeq platform (Illumina). Taxonomic annotation was carried out by using the Silva (release 138.1). The comparison of the relative abundance of taxa among different groups were performed by Student t-test. PICRUSt2 was used to perform microbial metabolic function prediction from 16S rRNA results (Douglas et al., 2020).

2.6 Statistical analysis

One-way Analysis of Variance (ANOVA) was tested for significance between the intervention groups and followed by Tukey's HSD with Bonferroni corrections ($P<0.05$). Tamhane's T2 analysis was used when variances were not homogenous. A two-side hypergeometric test was used as the statistical test method and Benjamini−Hochberg was used as the FDR correction method in the metabolites KEGG enrichment analysis. OPLS-DA was not chosen due to permutation tests were failed to validate the model thus partial least squares discriminant analysis (PLS-DA) was applied in multivariate analysis using SIMCA-P+ (V12.0, Umetrics AB, UmeÅ, Sweden). The PLS-DA models were validated by permutation test (R^2Y-intercept<0.3–0.4 and $Q2Y$-intercept<0.05) (Eriksson, 2002) and cross-validated analysis of variance (CV-ANOVA) ($P<0.05$). Linear discriminant analysis (LDA) effect size (LEfSe) was used to discriminate differentially abundant bacterial taxa, bacterial taxa with LDA absolute value>2 were considered differentially abundant bacterial.

3. Results

3.1 Behavioral outcomes

In this study, behavioral outcomes in rats were shown in Figure 1. OFT revealed that deficiency in dietary n-3 FA for 4 weeks showed a trend of decrease in center distance (Figure 1B), distance percentage in center (Figure 1D), center times (Figure 1F), and center entries (Figure 1H), although the difference compared with n-3 adequate group (n3De vs Con) did not reach statistical significance due to the high deviation. However, sn2DHA group showed lower center distance and center entries compared to the Con group but not n3De group.

3.2 Effect of n-3 fatty acid deficient diet and supplementation with triacyclglycerols containing DHA at different positions on fecal metabolic profile

A total of 1,627 features were found after removing the peaks representing internal standards and the unidentified features. Table S3 shows the result of quantitative enrichment analysis based on the metabolites representing the changed KEGG pathways between the groups. The paired comparison between the groups n3De vs. Trip or n3De vs. sn2DHA did not show significant difference in KEGG pathways analysis. The metabolites mapped to those pathways and the statistical analysis among groups are shown in the Figure S1. Table 1 summarizes the significantly changed pathways and the metabolites contributing to distinguished pathways revealed by quantitative enrichment analysis in the n3De vs. Con, n3De vs. sn1DHA n3De vs. sn3DHA comparisons. Selected significantly changed metabolites in those pathways are shown in boxplots (Figure 2 A–T).

Compared to the Con group fed the diet with soybean oil, groups fed with peanut oil showed significantly changed pyrimidine metabolism (mainly driven by lower level of thymidine, dihydrouracil, and deoxyuridine; Figure 2A–C), steroid biosynthesis (24, 25 - dihydrolanosterol,

231 delta 8,14-sterrol, 2, 3-epoxysqualene, and obtusifoliol; Figure 2D–G; farnesyl pyrophosphate;
232 Figure 2H), ascorbate and aldarate metabolism (glucaric acid; Figure 2I), arginine and proline
233 metabolism (proline and ornithine; Figure 2J and K; arginine, hydroxyglutarate semialdehyde, and
234 4-guanidinobutanoic acid; Figure 2L–N), metabolism of xenobiotics by cytochrome P450
235 (glutathione episulfonium ions; Figure 2O), N-glycan biosynthesis (dolichyl β-D-glucosyl
236 phosphate and glucosamine-1-phosphate (glucosamine-1P); Figure 2P and Q), histidine
237 metabolism (3-methylhistidine; Figure 2R), fatty acid biosynthesis (lower level of caprylic acid
238 and higher level of palmitic acid; Figure 2S and T), and fatty acid metabolism (palmitic acid;
239 Figure 2T). Compared to the n3De group, feeding TAGs containing DHA at *sn*-1 position
240 significantly affected pyrimidine metabolism (thymidine and dihydrouracil; Figure 2A and B),
241 steroid biosynthesis, beta-alanine metabolism (dihydrouracil; Figure 2B), and pantothenate and
242 CoA biosynthesis (dihydrouracil and 4-phosphopantothenate; Figure 2B and U). Feeding TAGs
243 containing DHA at *sn*-3 position significantly affected beta-alanine metabolism (dihydrouracil;
244 Figure 2B) compared to the n3De group. No significantly changed metabolism pathway was
245 observed in Con/Trip and n3DE/sn2DHA comparisons. In addition, higher level of 4-
246 guanidinobutanoic acid (Figure 2N) in n-3 deficient groups (the n3De and Trip groups) was
247 significantly reversed in sn2DHA and sn3DHA groups. The affected pathways between the Con
248 group and DHA containing groups were pyrimidine metabolism, steroid biosynthesis, N-glycan
249 biosynthesis, ascorbate and aldarate metabolism, arginine and proline metabolism, valine, leucine
250 and isoleucine biosynthesis, and sphingolipid metabolism (Table S3). The affected pathway
251 between the Trip group and sn1DHA/sn3DHA groups is beta-alanine metabolism (Table S3).
252 There was no difference in the level of palmitic acid among groups fed on diet with peanut oil. No
253 significant difference in DHA level was observed in feces among the groups (Figure S2).

Since not all metabolites were mapped to the KEGG pathway, PLS-DA analysis, a supervised clustering method, was constructed to show group classification and to identify the most changed metabolites that contribute to the group classification. Parameters for validating PLS-DA models are shown in Figure S3. Figure 3A-L shows boxplots of selected metabolites that were significantly changed by the feeding as indicated by the multivariate analyses. PLS-DA score plot and loading plot (Figure S4, Model 1) generated from all groups showed a clear separation between the normal feed group (the Con group) and groups fed n-3 fatty acid deficient peanut-oil-based chow (n3De, Trip, sn1DHA, sn2DHA, and sn3DHA groups). The loading plot displays the correlation between metabolites and groups. The metabolites in circles contribute to the group separation. Those metabolites in the right circle such as thymidine, 13Z-docosenamide, and 2,3-dihydrodipicolinate (Figure 2A, 3C and 3D) were significantly higher in the Con group compared to the other groups. Those metabolites in the left circle with negative w*c value (loading coefficient) such as glucosamine-1P, N5-carboxy aminoimidazole ribonucleotide, and dimethylbenzimidazole (Figure 2Q, 3A and B) were lower in the Con group compared to the other groups fed with n-3 fatty acid deficient peanut-oil-based rodent chow.

To exclude the impact caused by compositional differences between the soybean oil and the peanut oil, as well as to acquire clear comparison among the groups fed with n-3 fatty acid deficient peanut-oil-based rodent chow, PLS-DA model (Model 2) was generated after exclusion of the Con group (Figure 4A–B), in which first component explaining 11.4% of the variation and second component explaining 8.8% of the variation. The first component separated the n3De group and Trip group from the sn1DHA, sn2DHA, and sn3DHA groups. Furthermore, the n3De group was clearly clustered in the fourth quadrant. In the loading plot, metabolites located in the right circle showed higher level in the n3De group such as 13Z-docosenamide, 2,3-dihydrodipicolinate,

277 phosphatidylinositol PI (16:1_18:1), phosphatidic acid PA (16:0_18:1), phosphatidylserine
278 PS(19:0_16:0), phosphatidylethanolamine PE (14:0_16:1), as well as 12-oxo-ETE (shown also in
279 Figure 3C-I) compared to DHA supplemented groups, whereas N5-carboxyaminoimidazole
280 ribonucleotide and dimethyl benzimidazole were lower in the n3De group and the Trip group
281 (shown also in Figure 3A–B) compared to DHA supplemented groups.
282 PLS-DA model 3 (Figure 4C–D) was performed by exclusion of n3De group from the model 2 to
283 find metabolites contributing to the classification of Trip, sn1DHA, sn2DHA, and sn3DHA groups,
284 in which first component explaining 11.6% of the variation and second component explaining 9.5%
285 of the variation. The metabolites PI (16:1_18:1), PA (16:0_18:1), 2-oxaloglutaric acid, 2,3-
286 dihydrodipicolinate, and phorbol 12,13-dibutanoate in the right circle were especially higher in the
287 Trip group, however, only changes of 2,3-dihydrodipicolinate and PA (16:0_18:1) (Figure 3D and
288 3F) reached significance. The metabolites such as sirohydrochlorin, lysoPE (18:0_0:0), N5-
289 carboxyaminoimidazole ribonucleotide, folate, and 5'-deoxyadenosine in the left circle were
290 especially lower in the Trip group compared to the DHA-fed groups (Figure 4D), in which only
291 N5-carboxyaminoimidazole ribonucleotide reached significance (Figure 3A).
292 A fourth PLS-DA model (Figure 4E–F) was performed by further exclusion of Trip group from
293 model 3 to find metabolites contributing to the classification among the three DHA-fed groups:
294 sn1DHA, sn2DHA, and sn3DHA. Although the permutation test and CV-ANOVA did not validate
295 the model 4 (R^2Y-intercept > 0.3–0.4; CV-ANOVA p-value > 0.05), score and loading plots still
296 can be utilized to indicate difference in metabolomics profiles among the groups. From PLS-DA
297 model (Figure 4E–F), the sn1DHA and sn3DHA groups were separated from each other by the
298 first component and sn2DHA group was slightly separated from sn1DHA and sn3DHA groups by
299 the second component. 2,3-Dihydrodipicolinate, deoxycholic acid (Figure 3D and K), and 4-

phosphopantothenate (Figure 2U) were lower whereas dimethylbenzimidazole and 7-methyliric acid (Figure 3B and 3L) were higher in the sn3DHA group compared to other DHA-fed groups. The content of scopolamine was higher in the sn2DHA group than in the sn1DHA and sn3DHA groups (Figure 3J).

3.3 Effect of dietary n-3 fatty acids deficiency and triacyclglycerols containing DHA at different position on fecal microbiota

To address the role of n-3 FA-deficiency diet and TAGs containing DHA at different position on the gut microbial community, fecal gut microbiota taxa were identified using 16s rRNA sequencing. The richness and diversity of gut microbial composition were shown in Figure 5A-D. No significant difference was observed among the groups in gut microbial diversity measured as Shannon index, Simpson, ACE, and Chao1. The n-3 adequate Con group showed a non-significantly lower ratio of Firmicutes to Bacteroidetes compared to other groups (Figure 5E).

Fecal microbial composition heatmap and fecal microbial composition at phylum, class, family, and genus level were shown in Figure 5F-J. To determine whether any taxa at different taxonomic levels were enriched or depleted by n-3 deficiency diet and to detect potentially different impact by dietary supplementation with TAGs containing DHA at different position, the linear discriminant analysis (LDA) effect size (LEfSe) was calculated to pinpoint the main different features at all taxa (Figure 6).

Genera *Methanosarcina*, *Virgibacillus*, *Robinsonella*, *Gemmiger* and species *Ruminococcus bromii* were enriched in the n3De group compared to the Con group, whereas the genera *Chryseobacterium, Pseudomnas, Pyramidobacter*, *Alistips* and species *Parabacteroides distasonis* and *Bacteroides massiliensis* were depleted in the n3De group compared to the Con group (Figure 6). The number of significantly changed taxa was less in the Trip/n3De and n3De/sn1DHA

comparisons than in the comparison between n3De/sn2DHA as well as n3De/sn3DHA, indicating that the n3De, Trip, and sn1DHA groups shared similar gut microbiota taxa profile. This finding was also verified by the heatmap (Figure 5F) showing that the gut microbiota profile of n3De, Trip, and sn1DHA were clustered together by Ward clustering method. The abundance of species *Prevotella* sp. CAG: 1031 was decreased in all the three DHA groups compared to the n3De group. Only the groups fed TAGs containing DHA at *sn*-2 and *sn*-3 positions showed lower abundance of the genus *Ruminococcus* and species *Ruminococcus flavefaciens* compared to the n3De group. The sn2DHA group showed higher abundance of genus *Bacteroides* and species *Bacteroides fragilis* as well as lower abundance of genus *faecalibacterium* and species *faecalibacterium* sp. CAP 74 compared to the n3De group. LEfSe analyses in other comparisons were shown in Figure S5, the relative abundance of genus *Dorea* was higher in the Trip group compared to the sn1DHA, sn2DHA, and sn3DHA groups. And there were no differentiated gut microbiota taxa found in sn2DHA/sn3DHA comparison, suggesting similar gut microbiota taxa profile.

Function prediction of the gut microbiota revealed by PICRUSt2 showed comparisons of relative abundance levels of the KEGG pathway (Figure 7 and Figure S6). Biosynthesis of secondary metabolites, glycerolipid metabolism, and carbapenem biosynthesis were significantly different in Con/n3De comparison (Figure 7A). Feeding tripalmitin also affected gut microbiota metabolic pathways. For example, biosynthesis of secondary metabolites, phosphotransferase system, and pentose phosphate pathway were changed in the Trip group compared to the n3De group (Figure 7B). Compared to the n3De group, sn2DHA and sn3DHA showed different changes in KEGG pathway (Figure 7C-D). In sn2DHA group, the pathways in starch and sucrose metabolism and histidine metabolism was altered, whereas the sn3DHA group showed affected phosphotransferase

345 system, pentose phosphate pathway, and protein export. No changed pathway was detected in
346 sn1DHA/n3De comparison.

347 **3.4 Correlation between gut metabolites**

348 Correlation analysis was made between gut microbiota and metabolites. However, no correlation
349 ($r < -0.5$ or $r > 0.5$) was found between gut bacterial species and gut metabolites and between gut
350 metabolites and the predicted functions. Among gut microbiota only positive correlations were
351 found at species level within *Bacteroides* genus (Table S4). Certain selected correlation plots
352 between gut metabolites are shown in Figure 8. Palmitic acid was found to be positively correlated
353 with certain fatty acids (stearidonic acid, heptadecanoic acid, and heptanoic acid) (Figure 8A-C)
354 and negatively correlated lysoPI (16:1_0:0) and PI (18:1_18:1) (Figure 8D-E). α-Linolenic acid
355 was correlated with inositol-P-ceramide C (C26), diacylglycerol (16:1_16:1_0:0), and
356 diaminopimelic acid (Figure 8F-H). Dolichyl β-D-glucosyl phosphate was positively correlated
357 with glucosamine-1P (Figure 8I).

358 **4. Discussion**

359 The present study was conducted to investigate the impact of a four-week feeding with n-3 FA
360 deficient diet in the form of peanut-oil-based rodent chow and dietary supplementation of TAGs
361 possessing DHA either in *sn*-1, *sn*-2 or *sn*-3 position and two palmitic acid residues in the
362 remaining *sn*-positions on fecal metabolites and gut microbiota in rats.

363 Fecal content of DHA and palmitic acid is of interest since previous research has shown positive
364 impact of dietary DHA (Costantini et al., 2017), whereas dietary intake of *sn*-1/*sn*-3 palmitic acid
365 may increase the formation of calcium soap reducing the fat absorption and having negative impact
366 on gut microbiota (Wang et al., 2021). Dietary intake of saturated fatty acids was shown to reduce
367 the diversity of gut microbiota in humans (Schoeler et al., 2023). In this study, no significant

368 difference in fecal DHA level was observed among the groups. Previously in a 5-day intervention
369 feeding, fecal DHA level was slightly lower in the group fed with TAG containing DHA at *sn*-2
370 position compared to the groups fed with DHA at *sn*-1/3 positions (Linderborg et al., 2019).
371 Despite additional intake of palmitic acid in the Trip and DHA-fed groups, there are no significant
372 difference in fecal content of palmitic acid among the groups. These could have partially been
373 ascribed to the low efficiency of methanol overall for extracting lipids.
374 Quantitative pathway enrichment analysis was performed. We found metabolites thymidine,
375 dihydrouracil, and deoxyuridine involved in the pyrimidine metabolism pathway were higher in
376 the n-3 adequate Con group compared to all other groups. Disorders of brain pyrimidine
377 metabolism have been extensively reviewed to be related to neurological diseases such as sleep
378 disorders and Parkinson's disease, fecal pyrimidine metabolism might affect brain pyrimidine
379 metabolism through gut-brain axis (Vincenzetti et al., 2016). Recently fecal pyrimidine
380 metabolism has also been reported to be associated with brain function. Feeding dietary prebiotics
381 to stressed mice with sleep disorder has increased fecal pyrimidine nucleotides and improved sleep
382 disorder (Thompson et al., 2020). However, contrary results have shown a positive association
383 between metabolites involved in fecal pyrimidine metabolism (such as thymidine) and aberrant
384 brain connectivity in patients with irritable bowel syndrome (Osadchiy et al., 2020). In this study,
385 feeding TAGs containing DHA at *sn*-1 position regulated pyrimidine metabolism by mainly
386 increasing thymidine and dihydrouracil and feeding TAG containing DHA at *sn*-3 position also
387 reversed dihydrouracil level to the normal level, indicating a possible improved brain function,
388 although there were no beneficial changes in OFT. Although the mechanisms for how fecal
389 metabolites affect complex brain functions remain unknown, these data strongly support the
390 relationships between fecal pyrimidine metabolism, brain function, and n-3 FA-deficient status.

391 4-Guanidinobutanoic acid and arginine are involved in arginine and proline metabolism. Increased
392 4-guanidinobutanoic acid in serum could promote the production of ROS and indicated impaired
393 nerve system (Zhao et al., 2022). 4-Guanidinobutanoic acid level was increased in the n3De and
394 Trip groups compared to the Con group, feeding TAGs containing DHA decreased its level. The
395 n3De and Trip groups did not show altered arginine level compared to the Con groups and feeding
396 TAGs containing DHA increased the arginine level compared to n3De group. These results
397 potentially indicated an improved arginine and proline metabolism by supplementation of TAGs
398 containing DHA. Arginine plays an essential role not only in amino acid metabolism and the
399 growth hormones release, it is also the precursor for the nitric oxide (NO) which is produced by
400 the NO synthase, and gut microbiota has been reported to be capable of producing NO (Piva et al.,
401 2002; Vermeiren et al., 2009). Increased fecal arginine level in the groups fed with TAGs
402 containing DHA could possibly affect the NO level and immune system in the rats.
403 Multivariate analysis also revealed metabolites that contribute to the different metabolic profile in
404 groups. Glucosamine-1P is an important intermediate in formation of peptidoglycans as
405 components of bacteria cell wall (Ruscitto & Sharma, 2018). Increased of glucosamine-1P
406 indicated that n-3 FA deficiency diet affected gut microbiota activity in rats. N5-carboxy
407 aminoimidazole ribonucleotide which plays a center role in *de novo* purine biosynthesis in
408 microbes was increased in the n-3 deficient (n3De) group compared to the Con group. Feeding
409 tripalmitin to rats on top of n-3 FA deficient diet further increased its level. Moreover, feeding
410 TAG containing DHA also increased its level compared to the Trip group with sn3DHA group
411 showing the highest level of N5-carboxy aminoimidazole ribonucleotide followed by sn2DHA
412 group and then sn1DHA group. These results possibly indicated different dietary DHA-containing
413 TAGs affected purine metabolism differently especially those TAGs containing DHA at *sn*-2 and

414 *sn*-3 positions. Genes involved in vitamin B12 production has been identified in gut bacterial
415 genomes (Balabanova et al., 2021). In a bacteria culturing study, the supplementation of medium
416 with dimethylbenzimidazole, a lower ligand in the α-position of vitamin B12, has increased
417 vitamin B12 productivity of bacteria (Marwaha et al., 1983). In this study, feeding TAG containing
418 DHA especially at *sn*-3 position largely increased dimethylbenzimidazole level compared to other
419 DHA-fed groups, indicating a possibly more active vitamin B12 metabolism in these groups.
420 In gut bacteria, the level of 2,3-dihydrodipicolinate mainly depends on two major enzymes:
421 dihydrodipicolinate reductase and dihydrodipicolinate synthase. Both enzymes are involved in
422 lysine biosynthesis, in which dihydrodipicolinate synthase catalyzes the first step in the pathway
423 for the biosynthesis of lysine (Karsten et al., 2018). In a *Akkermansia muciniphila* culturing study,
424 mucin supplement-induced glycolysis metabolites production, which downregulated the
425 expression of dihydrodipicolinate reductase and thereby affect the 2,3-dihydrodipicolinate level
426 (Liu et al., 2021). 2,3-Dihydrodipicolinate was higher in the Con group compared to the n3De
427 group. Feeding TAGs further lowered this level, among which the sn3DHA group showed the
428 lowest level followed by the sn2DHA group and then the sn1DHA and Trip groups. These results
429 suggested n-3 FA-deficient peanut-oil-based diet and feeding fatty acids (in this case, DHA and
430 palmitic acid) in different positions of TAGs possibly affected lysine metabolism and mucin
431 degradation in gut differently.
432
433 12-Oxo-ETE has been reported to be related to the inflammation formation that occurs at sites
434 where its level increases to abnormal amounts such as in human rheumatoid arthritis, inflammatory
435 bowel disease etc. (Porro et al., 2014). Feeding TAGs containing DHA lowered the 12-oxo-ETE
436 level. Scopolamine is a nonselective muscarinic antagonist that has shown relatively rapid

antidepressant effects, although to date the findings are available from only limited clinical studies. Scopolamine reportedly has downstream signaling effects thought to be linked to neuroplasticity within glutamatergic synapses and consequent antidepressant action (Drevets et al., 2020). In this study, scopolamine was higher in the sn2DHA group compared to other groups, whereas no difference was found between Con and n3De groups. The Sn2DHA group showed highest level of deoxycholic acid, indicating altered bile acid reabsorption or production from cholesterol (Yu et al., 2021).

In this study, difference in gut microbiota was observed between rats fed with n-3 FA-deficient diet in the form of peanut-oil-based rodent chow and n-3 FA-adequate diet in the form of soybean-oil-based rodent chow, although gut microbial diversity and Firmicutes/Bacteroidetes (an indicator of intestinal dysbiosis) were not altered among groups. *Robinsoniella* and *Gemmiger* were enriched, whereas *Pseudomonas pyramidobacter* and *Parabacteroides distasonis* were depleted in the n-3 deficient n3De group compared to the n-3 adequate Con group. *Robinsonella* has been reported to be positively correlated with human fatty liver disease (Raman et al., 2013) and *Gemmiger* has been shown at higher level in the gut of patients with ulcerative colitis (Nishino et al., 2018). *Pseudomonas pyramidobacter* has been shown to be lower in patients with chronic kidney disease and colorectal cancer (Gao et al., 2015). *Parabacteroides distasonis* has been reported to be lower in patients with liver cirrhosis (Qin et al., 2014)**.** These results indicated n-3 FA-deficient peanut-oil-based diet might increase the risk of these diseases through modification of gut microbiota. Genera *Alistipes* and species *Bacteroides massiliensis,* which have been recorded at lower level in patients with mild cognitive impairment or Alzheimer's disease (Li et al., 2019; Petrov et al., 2017), was depleted in the n3De group compared to the n-3 adequate Con group, suggesting n-3 PUFA deficiency in the diet might affect brain function through the gut-

brain axis. Dietary flaxseed oil rich in α-linolenic acid, a n-3 essential fatty acid also present in soybean oil, has been reported to enrich *Alistipes* in the diabetic mice (Zhu et al., 2020). However, feeding TAGs containing DHA did not affect the abundance of *Alistipes.*

Feeding TAGs containing DHA decreased abundance of species *Prevotella* sp. CAG: 1031 compared to the n3De group. *Prevotella* sp. CAG: 1031 has been reported to be higher in lean pigs compared to fat pigs (Zhao et al., 2022) and lower in obese mice (Si et al., 2018). Metagenomics analysis showed *Prevotella* sp. CAG: 1031 has highest copies of gene 8-amino-7-oxononanoate synthase [EC:2.3.1.47] (K00652) among the species in the gut of male mice, which is an enzyme involved in biotin metabolism. Biotin synthesis begins by hijacking the fatty acid synthetic pathway, the downregulation of biotin metabolism might affect fatty acid synthesis (Lin et al., 2010). Lower abundance of the species *Prevotella* sp. CAG: 1031 induced by feeding TAGs containing DHA indicated lower biotin synthesis and possible impact on fatty acid metabolism in the DHA-supplemented groups.

Different doses of n-3 polyunsaturated FAs have been reported to affect gut microbial taxa in mice (Zhu et al., 2021). In this study, however, DHA at different positions in TAG showed also varying effect enriching or depleting gut microbiota taxa. In this study, only the groups fed with TAGs containing DHA at *sn*-2 and *sn*-3 positions decreased the genus *Ruminococcus* and the species *R. flavefaciens* compared to the n3De group. In a study exploring involvement of gut microbiota in antidepressant properties of DHA, positive correlation has been found between abundance of *Ruminococcus* and depressive behavior of mice (Davis et al., 2017). *R. flavefaciens* has been studied in depth in depressive behavior, showing that antidepressants could reduce the abundance of *R. flavefaciens*, feeding *R. flavefaciens* to depressed mice diminished antidepressants-induced

483 decrease in depressive behavior by inducing changes in cortical gene expression, up-regulating
484 genes involved in mitochondrial oxidative phosphorylation, while down-regulating genes involved
485 in neuronal plasticity (Lukić et al., 2019). The result suggested the sn2DHA and sn3DHA groups
486 might have more potential to reduce risk of brain dysfunction by inducing positive changes to gut
487 microbiota.
488 The sn2DHA group also showed higher abundance of genus *Bacteroides* and species *B. fragilis* as
489 well as lower abundance of genus *Faecalibacterium* and species *Faecalibacterium* sp. CAP 74. A
490 review summarized that a few studies also showed some common changes in the gut microbiota
491 after n-3 PUFA supplementation, in particular, a decrease in *Faecalibacterium* often associated
492 with an increase in the *Bacteroidetes* (Costantini et al., 2017). Recent studies also have shown
493 similar observations. For example, dietary DHA-ethyl ester and n-3 PUFAs (mixture of DHA and
494 EPA) increased the *Bacteroides* abundance in the gut of rats and mice, respectively (Hosomi et al.,
495 2021; Zhu et al., 2021). We previously revealed DHA at *sn*-2 position in TAG has the higher
496 bioavailability compared to DHA at other positions (Linderborg et al., 2019). Higher
497 bioavailability of DHA at *sn*-2 position might induce higher abundance of *B. fragilis* and lower
498 abundance of *Faecalibacterium* sp. CAP 74. Administration of *B. fragilis* protected against
499 inflammatory colitis in mice (Mazmanian et al., 2008), and it also reduced activation of pathogenic
500 T cells and increased generation or expansion of T regulatory cells in the liver of mice (Sofi et al.,
501 2021). These indicates that the sn2DHA group might have improved immunity compared to other
502 groups.
503 Palmitic acid was found to be positively correlated with stearidonic acid, heptadecanoic acid, and
504 heptanoic acid. Palmitic acid has been reported to impair paracellular permeability and cell-cell
505 junctions (Hosomi et al., 2020). Those fatty acids positively correlated with palmitic acid could be

from impaired gut barrier, and/or metabolism of palmitic acid by gut microbiota. High level of palmitic acid might increase the palmitoylation of and activation of type II phosphatidylinositol 4-kinase (PI4KII) β, which can phosphorylate phosphatidylinositols. In this study, palmitic acid might promote phosphorylation of phosphatidylinositols (Qu et al., 2021), partly contributing to the negative correlation between palmitic acid, lysoPI (16:1_0:0), and PI (18:1_18:1) found in this study.

Diaminopimelic acid is a vital component of peptidoglycan, crucial for the synthesis of bacterial cell walls in many pathogenic bacteria (Jiao et al., 2022). In addition, diaminopimelic acid is a specific ligand of NOD1 that regulates the proinflammatory NOD1/RIP2/NF-kB signaling pathway (Jiao et al., 2022). We found that α-linolenic acid was negatively correlated with diaminopimelic acid, indicating possible regulation of gut microbiota. Pro-inflammatory compound dolichyl β-D-glucosyl phosphate was positively correlated with glucosamine-1P, which might have been due to the fact that dolichyl β-D-glucosyl phosphate and glucosamine-1P both play roles in the N-glycosylation pathway essential for glycoprotein biosynthesis.

5. Conclusion

The present study was conducted to determine the impact of n-3 FA-deficient diet in the form of peanut-oil-based rodent chow on gut metabolic and microbiota profiles as well as the effect of supplementation of TAGs possessing DHA either in *sn*-1, *sn*-2 or *sn*-3 position. Peanut-oil-based rodent chow affected several fecal KEGG pathways such as pyrimidine metabolism (thymidine, dihydrouracil, and deoxyuridine), steroid biosynthesis (2, 3-epoxysqualene, 24, 25 - dihydrolanosterol, delta 8,14-sterrol, obtusifoliol, and farnesyl pyrophosphate), and arginine and proline metabolism (4-guanidinobutanoic acid and arginine). N5-carboxy aminoimidazole ribonucleotide related to purine biosynthesis and dimethylbenzimidazole involved in vitamin B2

biosynthesis were increased by feeding TAGs containing DHA, especially DHA at the *sn*-3 position. Increased fecal arginine and decreased 4-guanidinobutanoic acid levels in the groups fed with TAGs containing DHA could possibly indicate the improved immune system and nerve system in the rats, respectively. Changes between groups in 2,3-dihydrodipicolinate related to mucin degradation and glucosamine-1P involved in formation of cell wall indicated altered by gut microbiota profile, which was verified by 16s rRNA sequencing. N-3 FA-deficient diet lowered the genus *Alistipes* and species *Bacteroides massiliensis*, which indicate a potential risk for mild cognitive impairment or Alzheimer's disease. This change was not reversed by addition of DHA. However, feeding TAGs containing DHA at either one of the three positions and palmitic acid in the remaining ones decreased the abundance of species *Prevotella* sp. CAG: 1031, and feeding TAGs containing DHA at the *sn*-2 position increased abundance of *Bacteroides fragilis* and decreased the abundance of *Faecalibacterium* sp. CAP 74. Only the groups fed with TAGs containing DHA at *sn*-2 and *sn*-3 positions showed lower abundance of the genus *Ruminococcus* and the species *R. flavefaciens* compared to the n3De group. The results indicate DHA at different position of TAG affected gut metabolites and microbiota differently.

Abbreviations Used

DHA, docosahexaenoic acid; FA, fatty acids; OFT, open field test; PLS-DA, partial least squares discriminant analysis; TAGs, triacylglycerols.

Author Contributions

Kang Chen: Conceptualization, Methodology, Formal analysis, Investigation, Data curation, Writing – original draft, Xuetao Wei and Jian Zhang: Methodology and Investigation (Animal feeding trial). Haraldur G. Gudmundsson: Methodology and Investigation (Synthesis of Structured

552 TAGs), Writing – review & editing. Gudmundur G. Haraldsson: Methodology, Investigation,
553 Resources (Synthesis of Structured TAGs), Writing – review & editing. Qinghai Sheng: Writing –
554 review & editing. Yumei Zhang: Conceptualization, Funding acquisition, Resources. Baoru Yang:
555 Conceptualization, Investigation, Funding acquisition, Resources, Project Administration,
556 Supervision, Validation, Writing – review & editing.

557 **Declaration of competing interest**

558 The authors declare that they have no known competing financial interests or personal
559 relationships that could have appeared to influence the work reported in this paper.

560 **Data availability**

561 Data will be made available on request.

562 **Funding sources**

563 The study was supported by the Research Council of Finland (formerly the Academy of Finland)
564 in two projects (Decision numbers: 310982 & 356891) and by the Finland-China Food and Health
565 Network as a global pilot program for research and innovation funded by the Ministry of Education
566 and Culture of Finland (2021-2024). The project was also supported by the key projects of Beijing
567 Science and Technology Committee (Decision No. D171100008017002)

568

569 **References**

570 Arteaga, O., Revuelta, M., Urigüen, L., Martínez-Millán, L., Hilario, E., & Álvarez, A. (2017).
571 Docosahexaenoic acid reduces cerebral damage and ameliorates long-term cognitive
572 impairments caused by neonatal hypoxia–ischemia in rats. *Molecular Neurobiology*, *54*(9),
573 7137–7155. https://doi.org/10.1007/S12035-016-0221-8/FIGURES/17

574 Balabanova, L., Averianova, L., Marchenok, M., Son, O., & Tekutyeva, L. (2021). Microbial and
575 genetic resources for cobalamin (Vitamin B12) biosynthesis: from ecosystems to industrial
576 biotechnology. *International Journal of Molecular Sciences*, *22*(9), 4522.
577 https://doi.org/10.3390/IJMS22094522
578 Carrière, F., Rogalska, E., Cudrey, C., Ferrato, F., Laugier, R., & Verger, R. (1997). *In vivo* and
579 *in vitro* studies on the stereoselective hydrolysis of tri- and diglycerides by gastric and
580 pancreatic lipases. *Bioorganic & Medicinal Chemistry*, *5*(2), 429–435.
581 https://doi.org/10.1016/S0968-0896(96)00251-9
582 Costantini, L., Molinari, R., Farinon, B., & Merendino, N. (2017). Impact of omega-3 fatty acids
583 on the gut microbiota. *International Journal of Molecular Sciences*, *18*(12), 2645. (no page
584 number, only paper id here. I will delete this in clean version)
585 https://doi.org/10.3390/IJMS18122645
586 Davis, D. J., Hecht, P. M., Jasarevic, E., Beversdorf, D. Q., Will, M. J., Fritsche, K., & Gillespie,
587 C. H. (2017). Sex-specific effects of docosahexaenoic acid (DHA) on the microbiome and
588 behavior of socially-isolated mice. *Brain, Behavior, and Immunity*, *59*, 38–48. (no issue
589 number) https://doi.org/10.1016/J.BBI.2016.09.003
590 Dong, R., Lin, H., Ding, Y., Chen, X., Shi, R., Yuan, S., Li, J., Zhu, B., Xu, X., Shen, W., Wang,
591 K., Ding, D., & He, N. (2022). Effects of docosahexanoic acid on gut microbiota and fecal
592 metabolites in HIV-Infected patients with neurocognitive impairment: A 6-month
593 randomized, double-blind, placebo-controlled trial. *Frontiers in Nutrition*, *8,* 756720.
594 https://doi.org/10.3389/FNUT.2021.756720/FULL
595 Dong, X., Yao, S., Deng, L., Li, H., Zhang, F., Xu, J., Li, Z., Zhang, L., Jiang, J., & Wu, W.
596 (2022). Alterations in the gut microbiota and its metabolic profile of PM2.5 exposure-

induced thyroid dysfunction rats. *Science of the Total Environment*, *838*(3), 156402. https://doi.org/10.1016/J.SCITOTENV.2022.156402

Douglas, G. M., Maffei, V. J., Zaneveld, J. R., Yurgel, S. N., Brown, J. R., Taylor, C. M., Huttenhower, C., & Langille, M. G. I. (2020). PICRUSt2 for prediction of metagenome functions. *Nature Biotechnology*, *38*(6), 685–688. https://doi.org/10.1038/s41587-020-0548-6

Drevets, W. C., Bhattacharya, A., & Furey, M. L. (2020). The antidepressant efficacy of the muscarinic antagonist scopolamine: Past findings and future directions. *Advances in Pharmacology*, *89*, 357–386. https://doi.org/10.1016/BS.APHA.2020.04.002

Duan, R. (2000). Enzymatic aspects of fat digestion in the gastrointestinal tract. Fat digestion and absorption. *AOAC Press*. https://books.google.com/books?hl=en&lr=&id=t5FNYzGEUDsC&oi=fnd&pg=PA25&ots=asTLMhwFk-&sig=N4r3KE_ppoAIC6Rixryu4CpFwyk

Eriksson, I. (2002). Multi- and megavariate data analysis principles and spplications. *Journal of Chemometrics*, *16*(5), 261–262. https://doi.org/10.1002/cem.713

Gao, Z., Guo, B., Gao, R., Zhu, Q., & Qin, H. (2015). Microbiota disbiosis is associated with colorectal cancer. *Frontiers in Microbiology*, *6*(2), 20. https://doi.org/10.3389/FMICB.2015.00020/ABSTRACT

Ghasemifard, S., Turchini, G. M., & Sinclair, A. J. (2014). Omega-3 long chain fatty acid "bioavailability": A review of evidence and methodological considerations. *Progress in Lipid Research*, *56*, 92–108. https://doi.org/10.1016/J.PLIPRES.2014.09.001

Gunstone, F. D., & Harwood, J. L. (2007). Occurrence and characterisation of oils and fats. *The Lipid Handbook with CD-ROM, Third Edition*, 37–142.

620 Hosomi, K., Kiyono, H., & Kunisawa, J. (2020). Fatty acid metabolism in the host and
621 commensal bacteria for the control of intestinal immune responses and diseases. *Gut*
622 *Microbes*, *11*(3), 276. https://doi.org/10.1080/19490976.2019.1612662
623 Hosomi, R., Matsudo, A., Sugimoto, K., Shimono, T., Kanda, S., Nishiyama, T., Yoshida, M., &
624 Fukunaga, K. (2021). Dietary eicosapentaenoic acid and docosahexaenoic acid ethyl esters
625 influence the gut microbiota and bacterial metabolites in rats. *Journal of Oleo Science*,
626 *70*(10), 1469–1480. https://doi.org/10.5650/JOS.ESS21189
627 Hull, M. A. (2011). Omega-3 polyunsaturated fatty acids. *Best Practice & Research Clinical*
628 *Gastroenterology*, *25*(4–5), 547–554. https://doi.org/10.1016/J.BPG.2011.08.001
629 Iverson, S. J., Sampugna, J., & Oftedal, O. T. (1992). Positional specificity of gastric hydrolysis
630 of long-chain n-3 polyunsaturated fatty acids of seal milk triglycerides. *Lipids*, *27*(11), 870–
631 878. https://doi.org/10.1007/BF02535866
632 Jiao, J., Liu, J., Li, Q., Zhang, G., Pan, C., Luo, F., Zhang, Q., Qi, B., Zhao, L., Yin, P., & Shang,
633 D. (2022). Gut microbiota-derived diaminopimelic acid promotes the nod1/rip2 signaling
634 pathway and plays a key role in the progression of severe acute pancreatitis. *Frontiers in*
635 *Cellular and Infection Microbiology*, *12*, 838340.
636 https://doi.org/10.3389/FCIMB.2022.838340/BIBTEX
637 Kalpio, M., Magnússon, J. D., Gudmundsson, H. G., Linderborg, K. M., Kallio, H., Haraldsson,
638 G. G., & Yang, B. (2020). Synthesis and enantiospecific analysis of enantiostructured
639 triacylglycerols containing n-3 polyunsaturated fatty acids. *Chemistry and Physics of Lipids*,
640 *231*(3), 104937. https://doi.org/10.1016/j.chemphyslip.2020.104937
641 Karsten, W. E., Nimmo, S. A., Liu, J., & Chooback, L. (2018). Identification of 2, 3-
642 dihydrodipicolinate as the product of the dihydrodipicolinate synthase reaction from

643 *Escherichia coli*. *Archives of Biochemistry and Biophysics*, *653*, 50–62.
644 https://doi.org/10.1016/J.ABB.2018.06.011
645 Kaur, G., Begg, D. P., Barr, D., Garg, M., Cameron-Smith, D., & Sinclair, A. J. (2010). Short-
646 term docosapentaenoic acid (22 : 5n-3) supplementation increases tissue docosapentaenoic
647 acid, DHA and EPA concentrations in rats. *British Journal of Nutrition*, *103*(1), 32–37.
648 https://doi.org/10.1017/S0007114509991334
649 Kristinsson, B., Linderborg, K. M., Kallio, H., & Haraldsson, G. G. (2014). Synthesis of
650 enantiopure structured triacylglycerols. *Tetrahedron Asymmetry*, *25*(2), 125–132.
651 https://doi.org/10.1016/j.tetasy.2013.11.015
652 La Rosa, F., Clerici, M., Ratto, D., Occhinegro, A., Licito, A., Romeo, M., Di Iorio, C., & Rossi,
653 P. (2018). The gut-brain axis in Alzheimer's disease and omega-3. A critical overview of
654 clinical trials. *Nutrients*, *10*(9), 1–17. https://doi.org/10.3390/nu10091267
655 Lehner, R., & Kuksis, A. (1993). Triacylglycerol synthesis by an sn-1,2(2,3)-diacylglycerol
656 transacylase from rat intestinal microsomes. *Journal of Biological Chemistry*, *268*(12),
657 8781–8786. https://doi.org/10.1016/S0021-9258(18)52942-2
658 Li, B., He, Y., Ma, J., Huang, P., Du, J., Cao, L., Wang, Y., Xiao, Q., Tang, H., & Chen, S.
659 (2019). Mild cognitive impairment has similar alterations as Alzheimer's disease in gut
660 microbiota. *Alzheimer's & Dementia*, *15*(10), 1357–1366.
661 https://doi.org/10.1016/J.JALZ.2019.07.002
662 Lin, S., Hanson, R. E., & Cronan, J. E. (2010). Biotin synthesis begins by hijacking the fatty acid
663 synthetic pathway. *Nature Chemical Biology*, *6*(9), 682–688.
664 https://doi.org/10.1038/nchembio.420

Linderborg, K. M., Kulkarni, A., Zhao, A., Zhang, J., Kallio, H., Magnusson, J. D., Haraldsson, G. G., Zhang, Y., & Yang, B. (2019). Bioavailability of docosahexaenoic acid 22:6(n-3) from enantiopure triacylglycerols and their regioisomeric counterpart in rats. *Food Chemistry*, *283*(1), 381–389. https://doi.org/10.1016/j.foodchem.2018.12.130

Liu, X., Zhao, F., Liu, H., Xie, Y., Zhao, D., & Li, C. (2021). Transcriptomics and metabolomics reveal the adaption of *Akkermansia muciniphila* to high mucin by regulating energy homeostasis. *Scientific Reports*, *11*(1), 1–13. https://doi.org/10.1038/s41598-021-88397-z

Lukić, I., Getselter, D., Ziv, O., Oron, O., Reuveni, E., Koren, O., & Elliott, E. (2019). Antidepressants affect gut microbiota and *Ruminococcus flavefaciens* is able to abolish their effects on depressive-like behavior. *Translational Psychiatry*, *9*(1), 1–16. https://doi.org/10.1038/s41398-019-0466-x

Marwaha, S. S., Sethi, R. P., & Kennedy, J. F. (1983). Influence of 5,6-dimethylbenzimidazole (DMB) on vitamin B12 biosynthesis by strains of propionibacterium. *Enzyme and Microbial Technology*, *5*(5), 361–364. https://doi.org/10.1016/0141-0229(83)90008-X

Mazmanian, S. K., Round, J. L., & Kasper, D. L. (2008). A microbial symbiosis factor prevents intestinal inflammatory disease. *Nature*, *453*(7195), 620–625. https://doi.org/10.1038/nature07008

Morley, N., & Kuksis, A. (1972). Positional specificity of lipoprotein lipase. *Journal of Biological Chemistry*, *247*(20), 6389–6393. https://doi.org/10.1016/S0021-9258(19)44705-4

Nishino, K., Nishida, A., Inoue, R., Kawada, Y., Ohno, M., Sakai, S., Inatomi, O., Bamba, S., Sugimoto, M., Kawahara, M., Naito, Y., & Andoh, A. (2018). Analysis of endoscopic brush

687 samples identified mucosa-associated dysbiosis in inflammatory bowel disease. *Journal of*
688 *Gastroenterology*, *53*(1), 95–106. https://doi.org/10.1007/S00535-017-1384-4/FIGURES/6
689 Osadchiy, V., Mayer, E. A., Gao, K., Labus, J. S., Naliboff, B., Tillisch, K., Chang, L., Jacobs, J.
690 P., Hsiao, E. Y., & Gupta, A. (2020). Analysis of brain networks and fecal metabolites
691 reveals brain–gut alterations in premenopausal females with irritable bowel syndrome.
692 *Translational Psychiatry*, *10*(1), 1–8. https://doi.org/10.1038/s41398-020-01071-2
693 Oshima, Y., Watanabe, T., Endo, S., Hata, S., Watanabe, T., Osada, K., & Takenaka, A. (2017).
694 Effects of eicosapentaenoic acid and docosahexaenoic acid on anxiety-like behavior in
695 socially isolated rats. *Bioscience, Biotechnology, and Biochemistry*, *82*(4), 716–723.
696 https://doi.org/10.1080/09168451.2017.1403888
697 Petrov, V. A., Saltykova, I. V., Zhukova, I. A., Alifirova, V. M., Zhukova, N. G., Dorofeeva, Y.
698 B., Tyakht, A. V., Kovarsky, B. A., Alekseev, D. G., Kostryukova, E. S., Mironova, Y. S.,
699 Izhboldina, O. P., Nikitina, M. A., Perevozchikova, T. V., Fait, E. A., Babenko, V. V.,
700 Vakhitova, M. T., Govorun, V. M., & Sazonov, A. E. (2017). Analysis of gut microbiota in
701 patients with Parkinson's disease. *Bulletin of Experimental Biology and Medicine, 162*(6),
702 734–737. https://doi.org/10.1007/S10517-017-3700-7
703 Piva, A., Prandini, A., Fiorentini, L., Morlacchini, M., Galvano, F., & Luchansky, J. B. (2002).
704 Tributyrin and lactitol synergistically enhanced the trophic status of the intestinal mucosa
705 and reduced histamine levels in the gut of nursery pigs. *Journal of Animal Science*, *80*(3),
706 670–680. https://doi.org/10.2527/2002.803670X
707 Porro, B., Songia, P., Squellerio, I., Tremoli, E., & Cavalca, V. (2014). Analysis, physiological
708 and clinical significance of 12-HETE: A neglected platelet-derived 12-lipoxygenase

709 product. *Journal of Chromatography B*, *964*, 26–40.
710 https://doi.org/10.1016/J.JCHROMB.2014.03.015
711 Qin, N., Yang, F., Li, A., Prifti, E., Chen, Y., Shao, L., Guo, J., Le Chatelier, E., Yao, J., Wu, L.,
712 Zhou, J., Ni, S., Liu, L., Pons, N., Batto, J. M., Kennedy, S. P., Leonard, P., Yuan, C., Ding,
713 W., &Li, L. (2014). Alterations of the human gut microbiome in liver cirrhosis. *Nature,*
714 *513*(7516), 59–64. https://doi.org/10.1038/nature13568
715 Qu, M., Zhou, X., Wang, X., & Li, H. (2021). Lipid-induced s-palmitoylation as a vital regulator
716 of cell signaling and disease development. *International Journal of Biological Sciences*,
717 *17*(15), 4223. https://doi.org/10.7150/IJBS.64046
718 Raman, M., Ahmed, I., Gillevet, P. M., Probert, C. S., Ratcliffe, N. M., Smith, S., Greenwood,
719 R., Sikaroodi, M., Lam, V., Crotty, P., Bailey, J., Myers, R. P., & Rioux, K. P. (2013). Fecal
720 microbiome and volatile organic compound metabolome in obese humans with
721 nonalcoholic fatty liver disease. *Clinical Gastroenterology and Hepatology*, *11*(7), 868-875.
722 https://doi.org/10.1016/J.CGH.2013.02.015
723 Ruscitto, A., & Sharma, A. (2018). Peptidoglycan synthesis in *Tannerella forsythia*: Scavenging
724 is the modus operandi. *Molecular Oral Microbiology*, *33*(2), 125–132.
725 https://doi.org/10.1111/OMI.12210
726 Schoeler, M., Ellero-Simatos, S., Birkner, T., Mayneris-Perxachs, J., Olsson, L., Brolin, H.,
727 Loeber, U., Kraft, J. D., Polizzi, A., Martí-Navas, M., Puig, J., Moschetta, A., Montagner,
728 A., Gourdy, P., Heymes, C., Guillou, H., Tremaroli, V., Fernández-Real, J. M., Forslund, S.
729 K., & Caesar, R. (2023). The interplay between dietary fatty acids and gut microbiota
730 influences host metabolism and hepatic steatosis. *Nature Communications*, *14*(1), 1–16.
731 https://doi.org/10.1038/s41467-023-41074-3

Si, Y. C., Miao, W. N., He, J. Y., Chen, L., Wang, Y. L., & Ding, W. J. (2018). Regulating gut flora dysbiosis in obese mice by electroacupuncture. *The American Journal of Chinese Medicine*, *46*(7), 1481–1497. https://doi.org/10.1142/S0192415X18500763

Sofi, M. H., Wu, Y., Ticer, T., Schutt, S., Bastian, D., Choi, H. J., Tian, L., Mealer, C., Liu, C., Westwater, C., Armeson, K. E., Alekseyenko, A. V., & Yu, X. Z. (2021). A single strain of *Bacteroides fragilis* protects gut integrity and reduces GVHD. *JCI Insight*, *6*(3), e136841. https://doi.org/10.1172/JCI.INSIGHT.136841

Swanson, D., Block, R., & Mousa, S. A. (2012). Omega-3 fatty acids EPA and DHA: health benefits throughout life. *Advances in Nutrition*, *3*(1), 1–7. https://doi.org/10.3945/AN.111.000893

Thompson, R. S., Vargas, F., Dorrestein, P. C., Chichlowski, M., Berg, B. M., & Fleshner, M. (2020). Dietary prebiotics alter novel microbial dependent fecal metabolites that improve sleep. *Scientific Reports*, *10*(1), 1–14. https://doi.org/10.1038/s41598-020-60679-y

Vermeiren, J., Van De Wiele, T., Verstraete, W., Boeckx, P., & Boon, N. (2009). Nitric oxide production by the human intestinal microbiota by dissimilatory nitrate reduction to Ammonium. *Journal of Biomedicine and Biotechnology*, 2009, 284718, https://doi.org/10.1155/2009/284718

Vincenzetti, S., Polzonetti, V., Micozzi, D., & Pucciarelli, S. (2016). Enzymology of pyrimidine metabolism and neurodegeneration. *Current Medicinal Chemistry*, *23*(14), 1408–1431. https://doi.org/10.2174/0929867323666160411125803

Wang, H., Chen, Z., Wang, M., Long, M., Ren, T., Chen, C., Dai, X., Yang, S., & Tan, S. (2022). The effect of polyphenol extract from rosa roxburghii fruit on plasma metabolome

and gut microbiota in type 2 diabetic mice. *Foods*, *11*(12), 1747. https://doi.org/10.3390/foods11121747

Wang, L., Bravo-Ruiseco, G., Happe, R., He, T., van Dijl, J. M., & Harmsen, H. J. M. (2021). The effect of calcium palmitate on bacteria associated with infant gut microbiota. *Microbiology Open*, *10*(3), e1187. https://doi.org/10.1002/MBO3.1187

Wang, X., Pan, L., Lu, J., Li, N., & Li, J. (2012). N-3 PUFAs attenuate ischemia/reperfusion induced intestinal barrier injury by activating I-FABP-PPARγ pathway. *Clinical Nutrition*, *31*(6), 951–957. https://doi.org/10.1016/J.CLNU.2012.03.003

Xiao, M., Xiang, W., Chen, Y., Peng, N., Du, X., Lu, S., Zuo, Y., Li, B., Hu, Y., & Li, X. (2022). DHA ameliorates cognitive ability, reduces amyloid deposition, and nerve fiber production in Alzheimer's disease. *Frontiers in Nutrition*, *9*, 852433. https://doi.org/10.3389/FNUT.2022.852433/BIBTEX

Yang, L. Y., Kuksis, A., & Myher, J. J. (1995). Biosynthesis of chylomicron triacylglycerols by rats fed glyceryl or alkyl esters of menhaden oil fatty acids. *Journal of Lipid Research*, *36*(5), 1046–1057. https://doi.org/10.1016/S0022-2275(20)39862-X

Yang, L. Y., Kuksis, A., & Myher, J. J. (2011). Intestinal absorption of menhaden and rapeseed oils and their fatty acid methyl and ethyl esters in the rat. *Biochemistry and Cell Biology, 68*(2), 480–491. https://doi.org/10.1139/O90-068

Yu, H., Fang, C., Li, P., Wu, M., & Shen, S. (2021). The relevance of DHA with modulating of host-gut microbiome signatures alterations and repairing of lipids metabolism shifts. *European Journal of Pharmacology*, *895*, 173885. https://doi.org/10.1016/J.EJPHAR.2021.173885

Zhao, G., Xiang, Y., Wang, X., Dai, B., Zhang, X., Ma, L., Yang, H., & Lyu, W. (2022). Exploring the possible link between the gut microbiome and fat deposition in pigs. *Oxidative Medicine and Cellular Longevity*, 2022, 1098892. https://doi.org/10.1155/2022/1098892

Zhao, Q., Fu, Y., Zhang, F., Wang, C., Yang, X., Bai, S., Xue, Y., Shen, Q., Zhao, Q., Fu, Y., Zhang, F., Wang, C., Xue, Y., Shen, Q., Yang, X., & Bai, S. (2022). Heat-treated adzuki bean protein hydrolysates reduce obesity in mice fed a high-fat diet via remodeling gut microbiota and improving metabolic function. *Molecular Nutrition & Food Research*, *66*(8), 2100907. https://doi.org/10.1002/MNFR.202100907

Zhu, L., Sha, L., Li, K., Wang, Z., Wang, T., Li, Y., Liu, P., Dong, X., Dong, Y., Zhang, X., & Wang, H. (2020). Dietary flaxseed oil rich in omega-3 suppresses severity of type 2 diabetes mellitus via anti-inflammation and modulating gut microbiota in rats. *Lipids in Health and Disease*, *19*(1), 1–16. https://doi.org/10.1186/S12944-019-1167-4/FIGURES/12

Zhu, X., Bi, Z., Yang, C., Guo, Y., Yuan, J., Li, L., & Guo, Y. (2021). Effects of different doses of omega-3 polyunsaturated fatty acids on gut microbiota and immunity. *Food & Nutrition Research*, *65*, 6263. https://doi.org/10.29219/FNR.V65.6263

Zhuang, P., Li, H., Jia, W., Shou, Q., Zhu, Y., Mao, L., Wang, W., Wu, F., Chen, X., Wan, X., Wu, Y., Liu, X., Li, Y., Zhu, F., He, L., Chen, J., Zhang, Y., & Jiao, J. (2021). Eicosapentaenoic and docosahexaenoic acids attenuate hyperglycemia through the microbiome-gut-organs axis in db/db mice. *Microbiome*, *9*(1), 185. https://doi.org/10.1186/s40168-021-01126-6

Figure 1. Behavioral outcomes in rats following dietary TAGs containing DHA at different position in the open field test. (A) Total distance; (B) Center distance; (C) Periphery distance; (D) Distance percentage in center; (E) Distance percentage in periphery; (F) Center time; (G) Periphery time; (H) Center entries; Note: * $p < 0.05$, ** $p < 0.01$, and *** $p < 0.001$

Figure 2. Selected significantly changed metabolites mapped to affected metabolic pathways. Bars with different letter differ from one another.

Figure 3. Selected significantly changed metabolites from multivariate analysis of all groups. Bars with different letters differ from one another.

Figure 4. PLS-DA score plot (A) and loading plot (B) based on identified metabolites from n3De, Trip, sn1DHA, sn2DHA, and sn3DHA groups. PLS-DA score plot (C) and loading plot (D) based on identified metabolites from Trip, sn1DHA, sn2DHA, and sn3DHA groups. PLS-DA score plot (E) and loading plot (F) based on identified metabolites from sn1DHA, sn2DHA, and sn3DHA groups.

Figure 5. Gut microbiota diversity indexes (A)-(D), the ratio of Firmicutes to Bacteroidetes (E), heatmap of gut microbiota abundances (F), fecal microbial composition at phylum (G), class (H), family (I), and genus (J) level.

Figure 6. Significantly changed gut microbes revealed by LEfSe (LDA Effect Size) in comparisons of Con/n3De, Trip/n3De, n3De/sn1DHA, n3De/sn2DHA, and n3De/sn3DHA. The unit of Y axis is relative intensities.

Figure 7. Extended error bar plot identifying significant altered KEGG pathway of gut microbiota in comparisons of Con/n3De, Trip/n3De, n3De/sn2DHA, and n3De/sn3DHA. The unit of Y axis is relative intensities.

Figure 8. Correlation plots between selected metabolites.

844 Figure 1

845

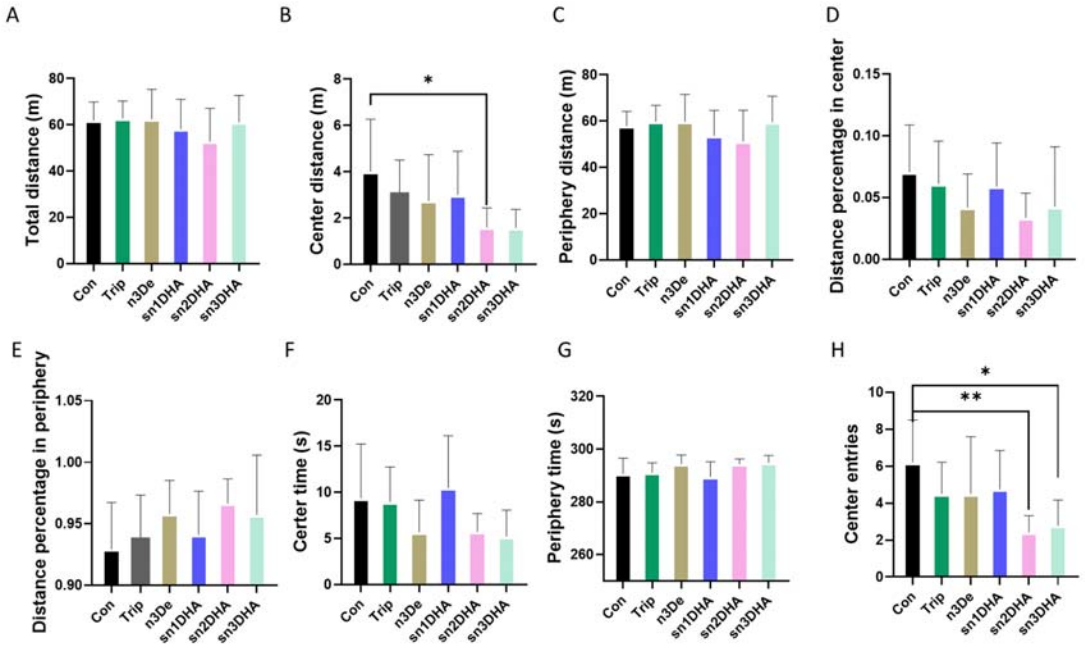

846

Figure 2

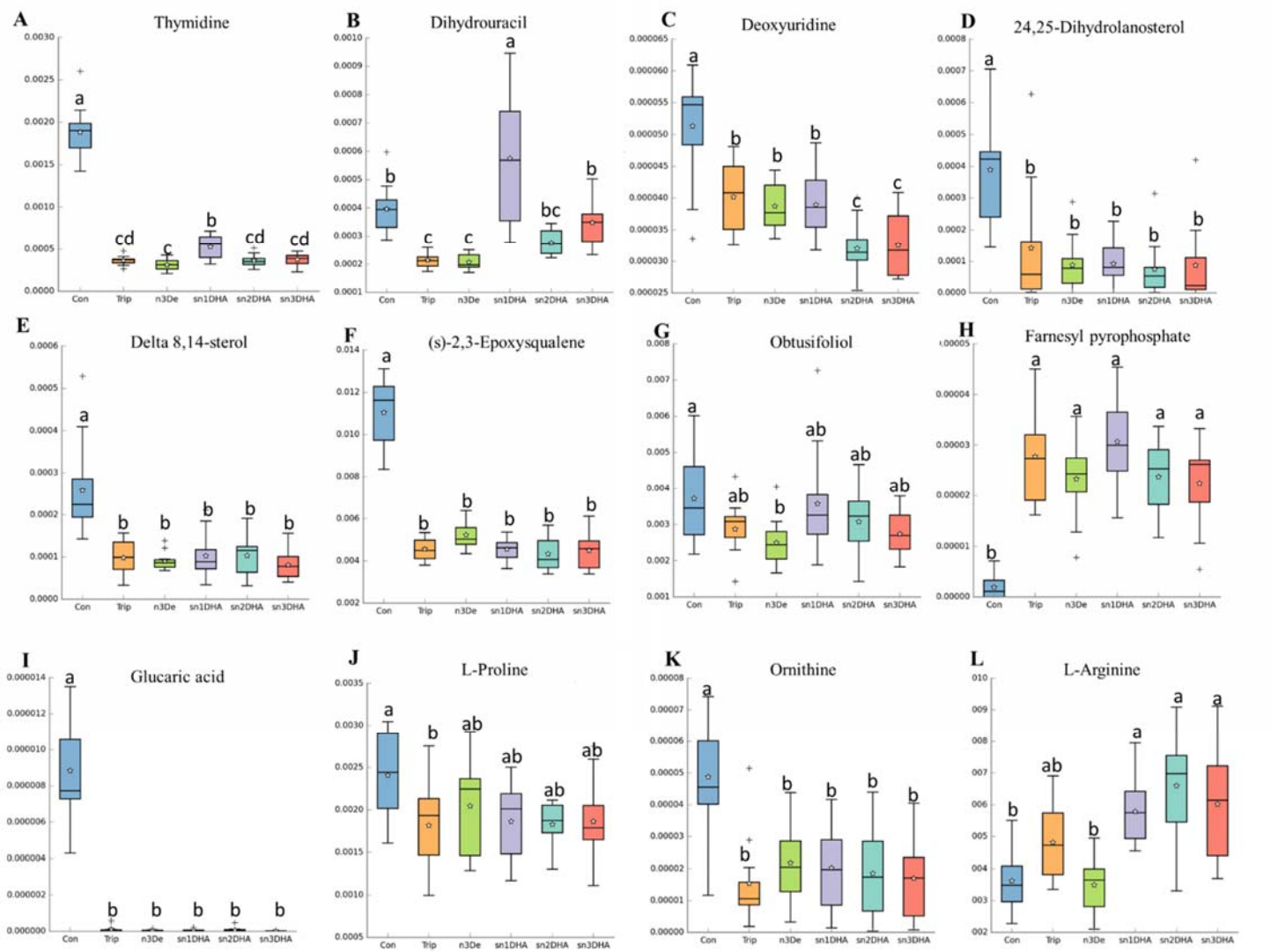
A
Thymidine
B
Dihydrouracil
C
Deoxyuridine
D
24,25-Dihydrolanosterol
E
Delta 8,14-sterol
F
(s)-2,3-Epoxysqualene
G
Obtusifoliol
H
Farnesyl pyrophosphate
I
Glucaric acid
J
L-Proline
K
Ornithine
L
L-Arginine
Con
Trip
n3De
sn1DHA
sn2DHA
sn3DHA

Supplementary

Effect of feed supplementation with docosahexaenoic acid in regio- and enantiopure triacylglycerols on gut metabolome and microbiota in rats

Kang Chen†, Xuetao Wei‡, Zhang Jian§, Haraldur G. Gudmundsson[#], Gudmundur G. Haraldsson[#], Qinghai Sheng[&], Yumei Zhang§*, Baoru Yang†*

†Food Sciences, Department of Life Technologies, University of Turku, FI-20014 Turun yliopisto, Finland

‡Beijing Key Laboratory of Toxicological Research and Risk Assessment for Food Safety, Department of Toxicology, School of Public Health, Beijing University, Beijing 100191, China

§Department of Nutrition and Food Hygiene, School of Public Health, Beijing University, Beijing 100191, China

[#] Science Institute, University of Iceland, IS-107 Reykjavik, Iceland

[&]College of Food Science and Technology, Hebei Agricultural University, Baoding 071001, China

* Author for Correspondence:

Professor Baoru Yang,

baoru.yang@utu.fi; Tel: +358 452737988

*Co-correspondence:

Professor Yumei Zhang

Email: zhangyumei@bjmu.edu.cn; Tel: +8613426134251

Table S1. Composition of diet

Ingredients	Contents (g/kg)
Corn starch	397
Casein (> 85% protein)	200
Corn dextrin (90–94% tetrose)	132
Sucrose	100
Oil[1]	70
Fiber	50
Minerals	35.5
Vitamins	10
L-cystinol	3
Choline bitartrate (42% choline)	2.5
Tert-butylhydroquinone	0.014

[1] Low n-3 FA diet (modified AIN-93G diet) for the n3De, Trip, sn1DHA, sn2DHA, and sn3DHA groups contained peanut oil. Standard n-3 AIN-93G diet for the Con group contained soybean oil

Table S2 Fatty acid composition of oils used in the feed. Values are expressed as mean mass percentages of two replicates.

Fatty acid	Soybean oil	Peanut oil
16:0	10.40	9.61
18:0	4.46	3.54
18:1(n-9)	22.95	49.75
18:2(n-6)	53.30	31.29
18:3(n-3)	7.50	0.11
20:0	0.40	1.24
22:0	0.40	2.39
24:0	0.12	1.04
Others[1]	0.47	1.03

[1] This category includes 16:1(n-7), 18:1(n-7), 18:3(n-6), 20:1(n-9) and 23:0.

TableS3 Summary table for the quantitative enrichment analysis ranked by Holm p-value. Holm p-value is the p-value adjusted by the Holm-Bonferroni test that is a method to counteract the problem of multiple comparisons and is widely used for large-scale data analysis. x indicates significant change.

	Con/n3DE	Con/Trip	Con/sn1DHA	Con/sn2DHA	Con/sn3DHA	n3DE/Trip	n3DE/sn1DHA	n3DE/sn2DHA	n3DE/sn3DHA	Trip/sn1DHA	Trip/sn2DHA	Trip/sn3DHA	sn1DHA/sn2DHA	sn1DHA/sn3DHA	sn2DHA/sn3DHA
Pyrimidine metabolism	x	x	x	x	x		x			x			x		
Steroid biosynthesis	x	x	x	x	x		x								
N-Glycan biosynthesis	x	x	x	x	x										
Ascorbate and aldarate metabolism	x	x	x	x	x										
beta-Alanine metabolism	x	x					x		x	x		x	x	x	
Metabolism of xenobiotics by cytochrome P450	x	x													
Histidine metabolism	x														
Arginine and proline metabolism	x	x	x	x	x										
Fatty acid degradation	x	x	x	x											
Fatty acid biosynthesis	x	x													
Fatty acid elongation	x	x													
Valine, leucine and isoleucine biosynthesis		x	x	x	x										
Glycerolipid metabolism		x			x										
Pantothenate and CoA biosynthesis		x					x			x					
Steroid hormone biosynthesis		x	x		x										
Fructose and mannose metabolism			x	x											
Sphingolipid metabolism			x	x	x										
Glycine, serine and threonine metabolism					x										

Table S4 Correlation analysis between gut microbiota at species level.

Correlation pairs	Correlation coefficient	P value
('Bacteroides_sp._AM16-15', 'Bacteroides_sp._CAG:98')	0.999591571	1.54356E-52
('Bacteroides_sp._AM22-3LB', 'Bacteroides_sp._CAG:98')	0.99962793	3.31526E-53
('Bacteroides_sp._AM16-15', 'Bacteroides_sp._AM22-3LB')	0.999748845	5.06544E-56
('Bacteroides_sp._AM16-15', 'Bacteroides_sp._AM25-34')	0.999754601	3.45552E-56
('Bacteroides_sp._AM25-34', 'Bacteroides_sp._CAG:98')	0.99977323	9.39371E-57
('Bacteroides_massiliensis', 'Bacteroides_sp._AM16-15')	0.999804403	8.1895E-58
('Bacteroides_massiliensis', 'Bacteroides_sp._CAG:98')	0.999831142	7.24371E-59
('Bacteroides_sp._AM22-3LB', 'Bacteroides_sp._AM25-34')	0.99984375	2.01344E-59
('Bacteroides_massiliensis', 'Bacteroides_sp._AM22-3LB')	0.999845795	1.62004E-59
('Bacteroides_massiliensis', 'Bacteroides_sp._AM25-34')	0.999892545	4.18085E-62

A Pyrimidine metabolism

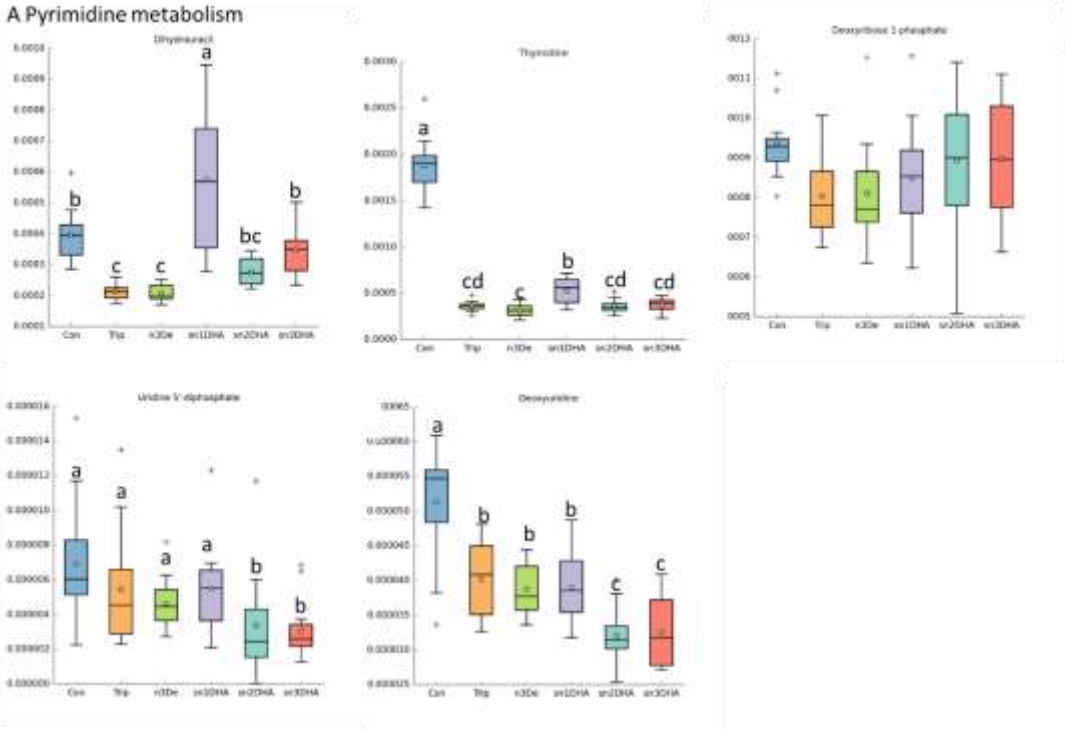

B Steroid biosynthesis

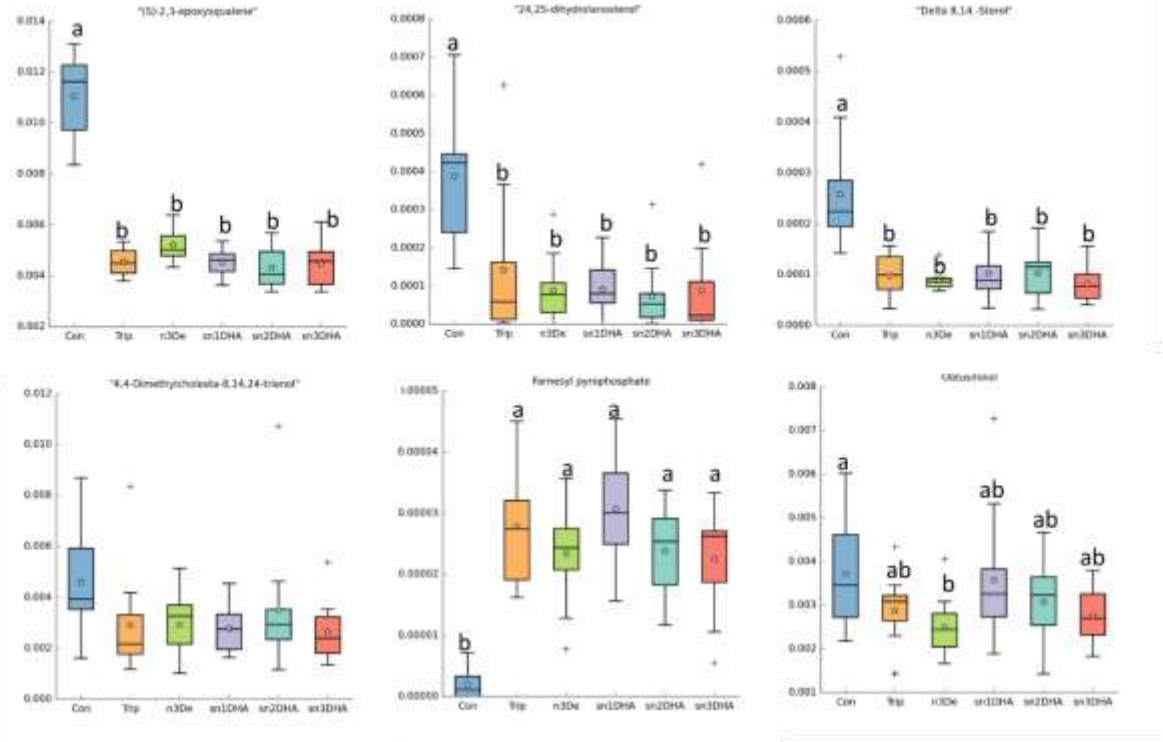

C N-Glycan biosynthesis

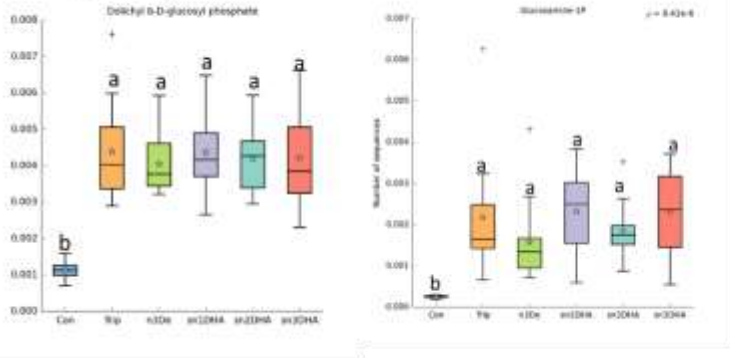

D Ascorbate and aldarate metabolism

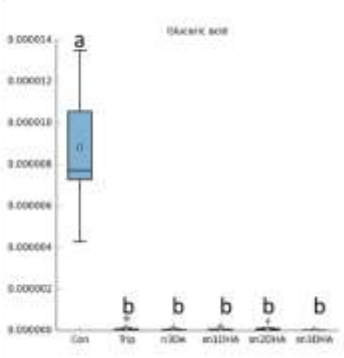

E beta-Alanine metabolism

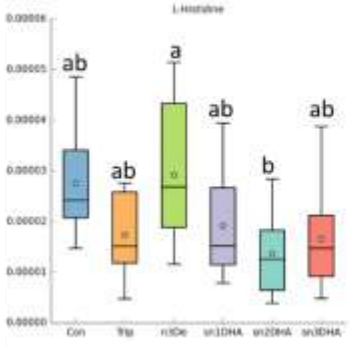

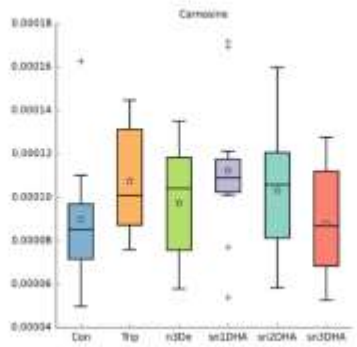

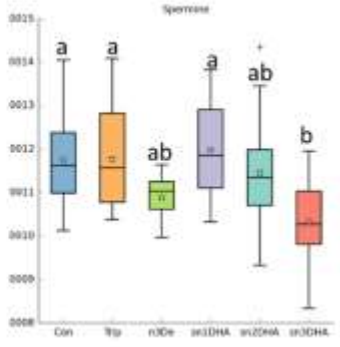

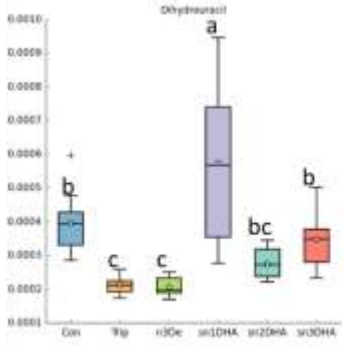

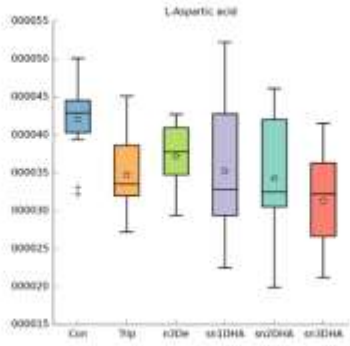

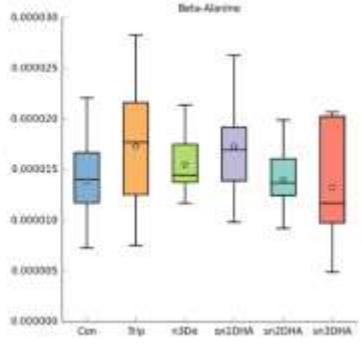

F Metabolism of xenobiotics by cytochrome P450

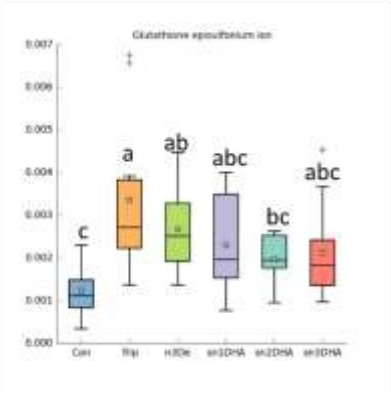

G Histidine metabolism

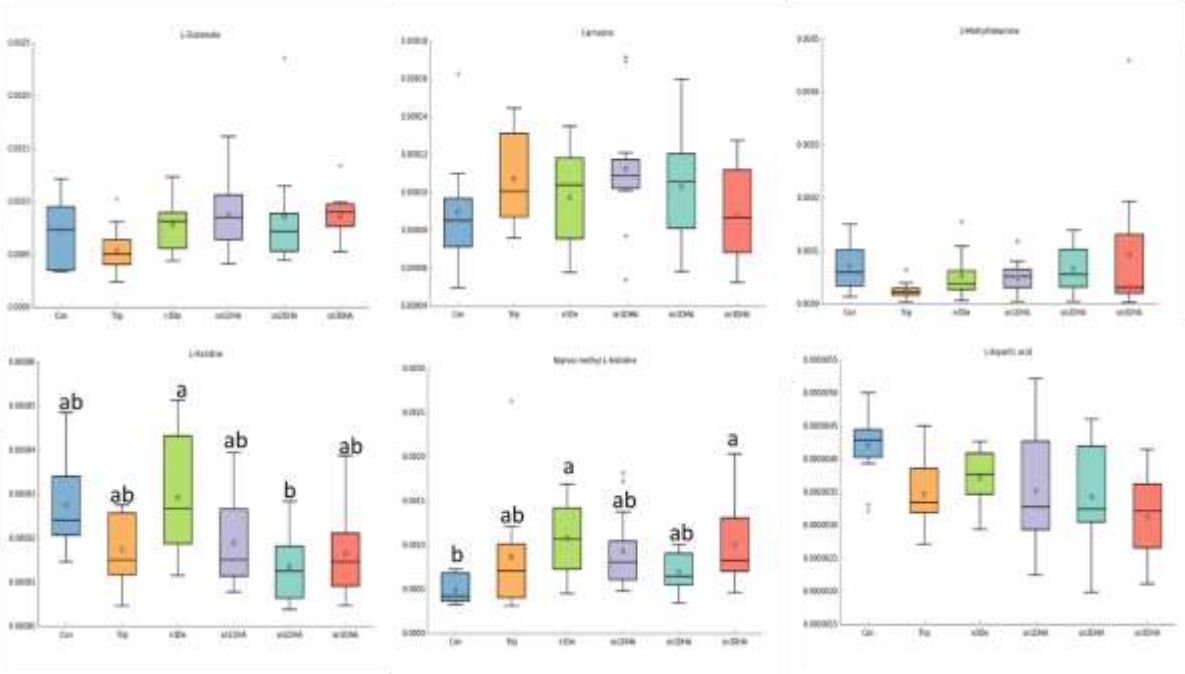

H Arginine and proline metabolism

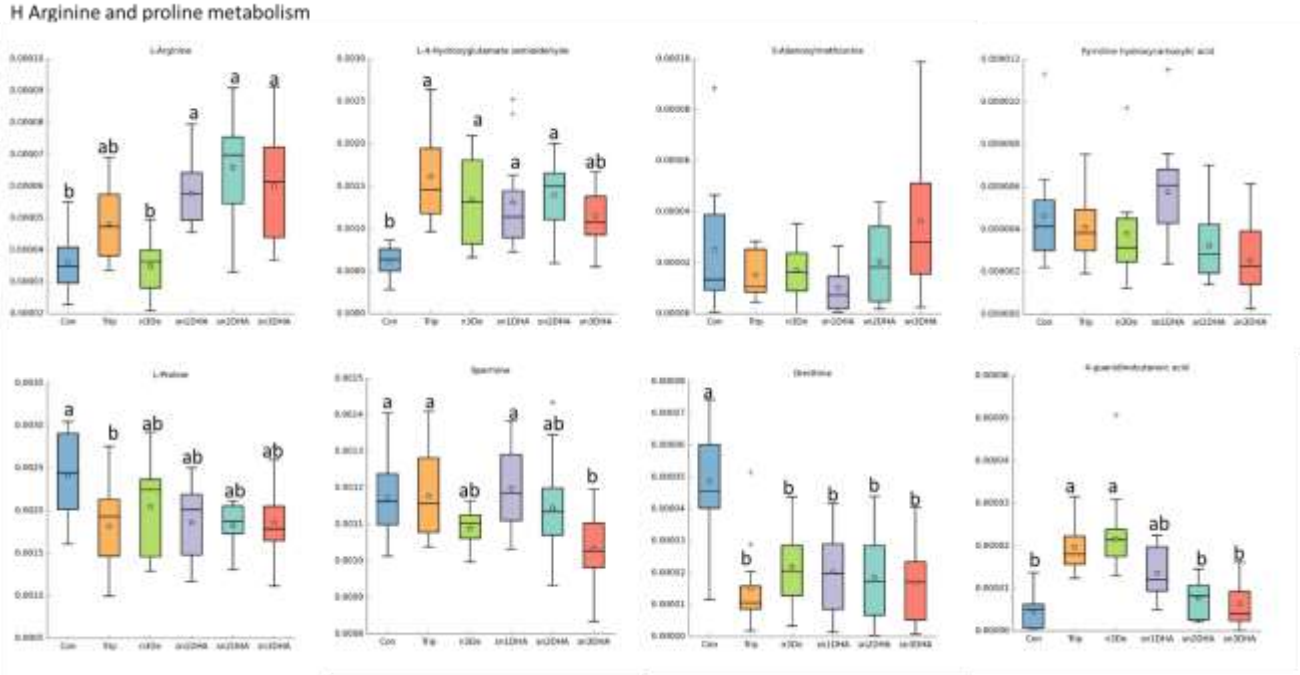

I Fatty acid degradation

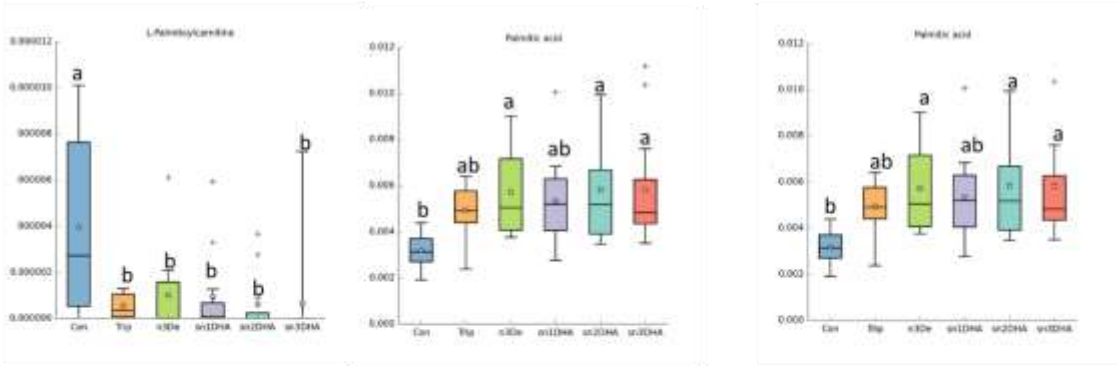

J Fatty acid biosynthesis

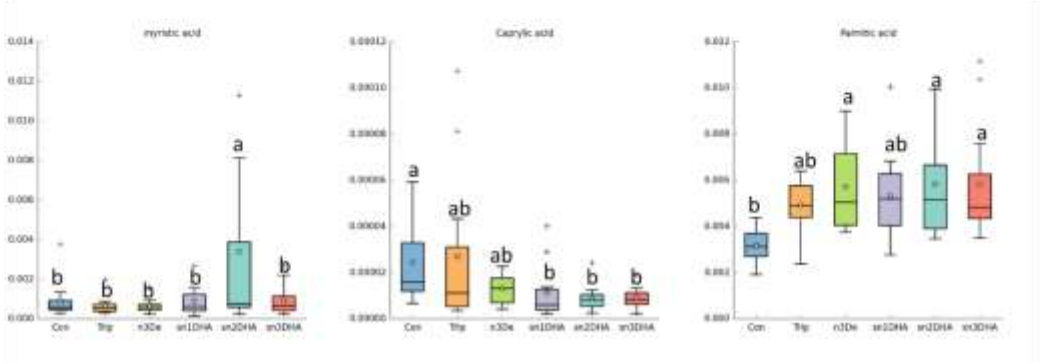

L Valine, leucine, and isoleucine metabolism

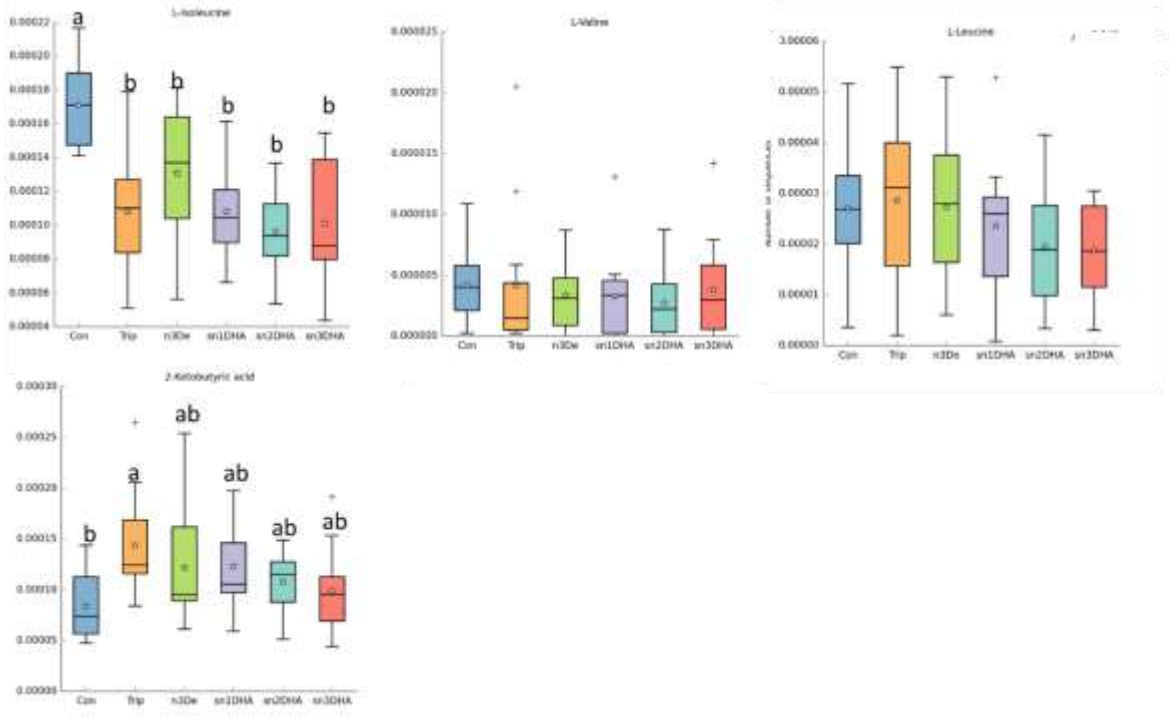

M Glycerolipid metabolism

N Pantothenate and CoA biosynthesis

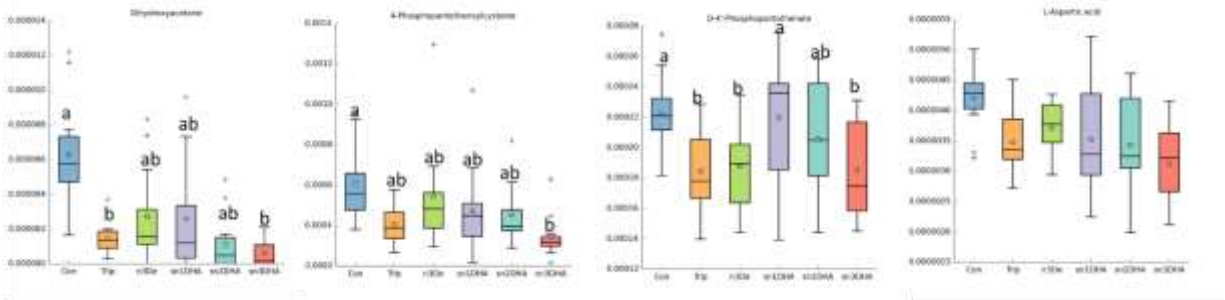

O Steroid hormone biosynthesis

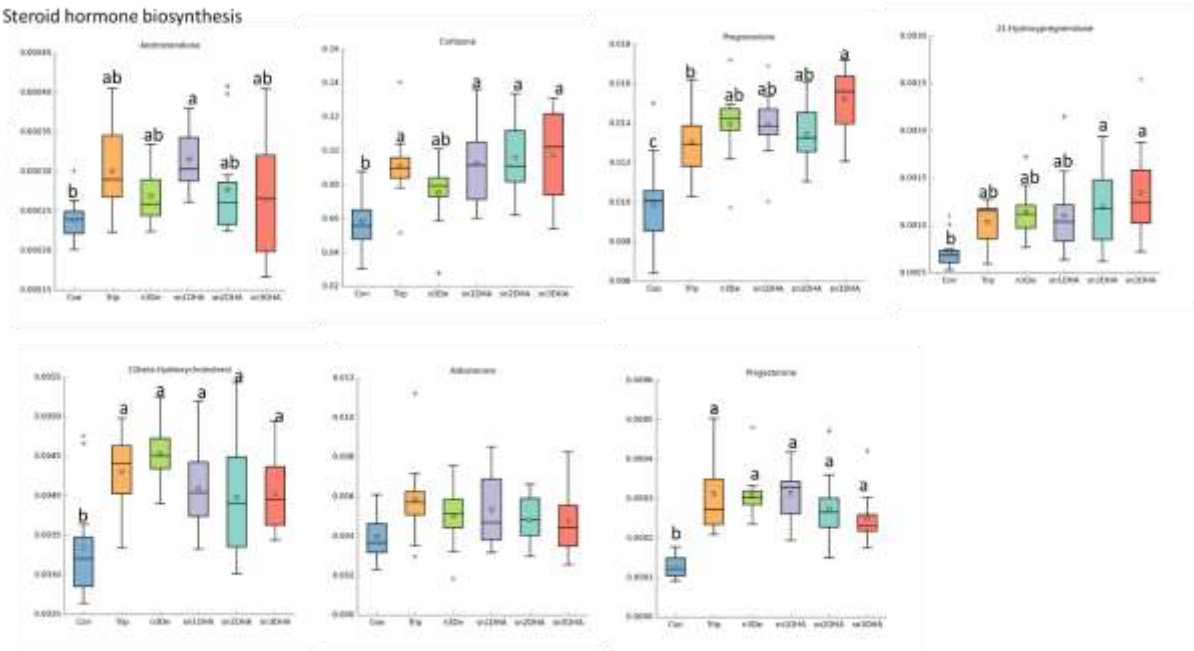

P Fructose and mannose metabolism

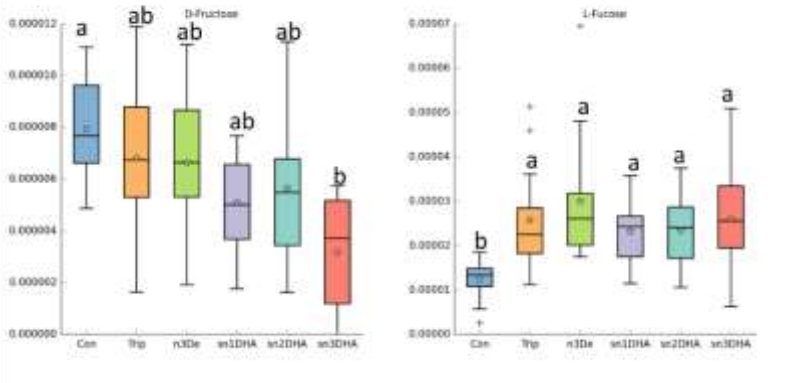

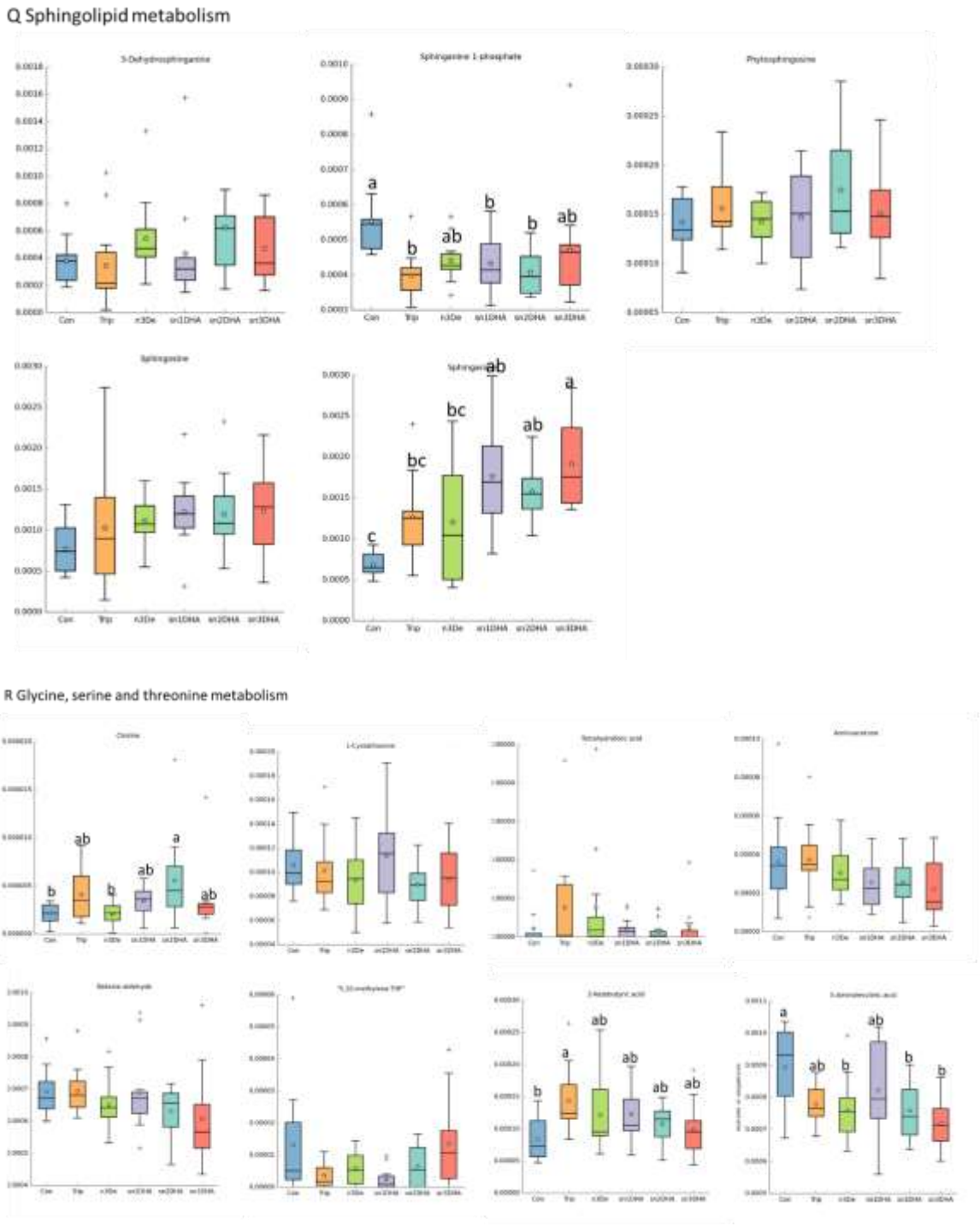

Figure S1. Metabolites mapped to those pathways in Table S3 and their statistical analysis.

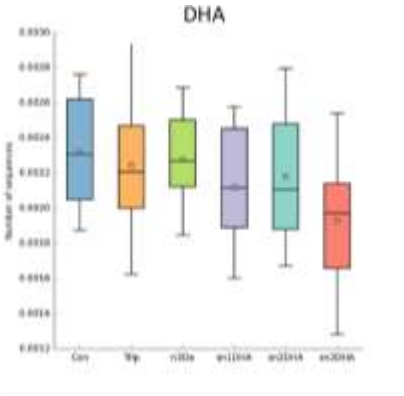

Figure S2. DHA level.

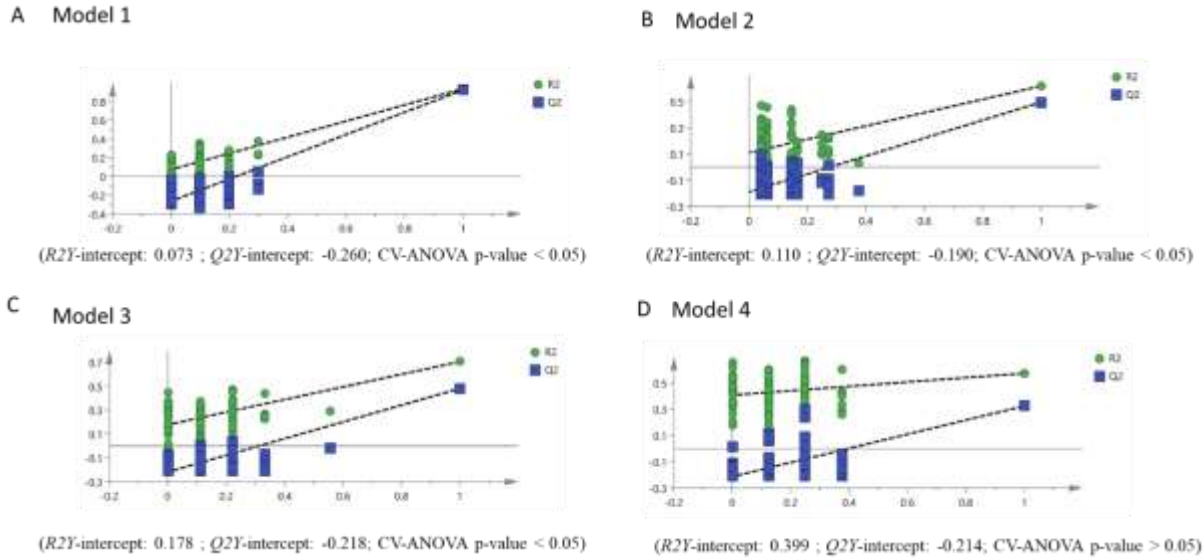

Figure S3. Validation of PLS-DA models by permutation test and CV-ANOVA.

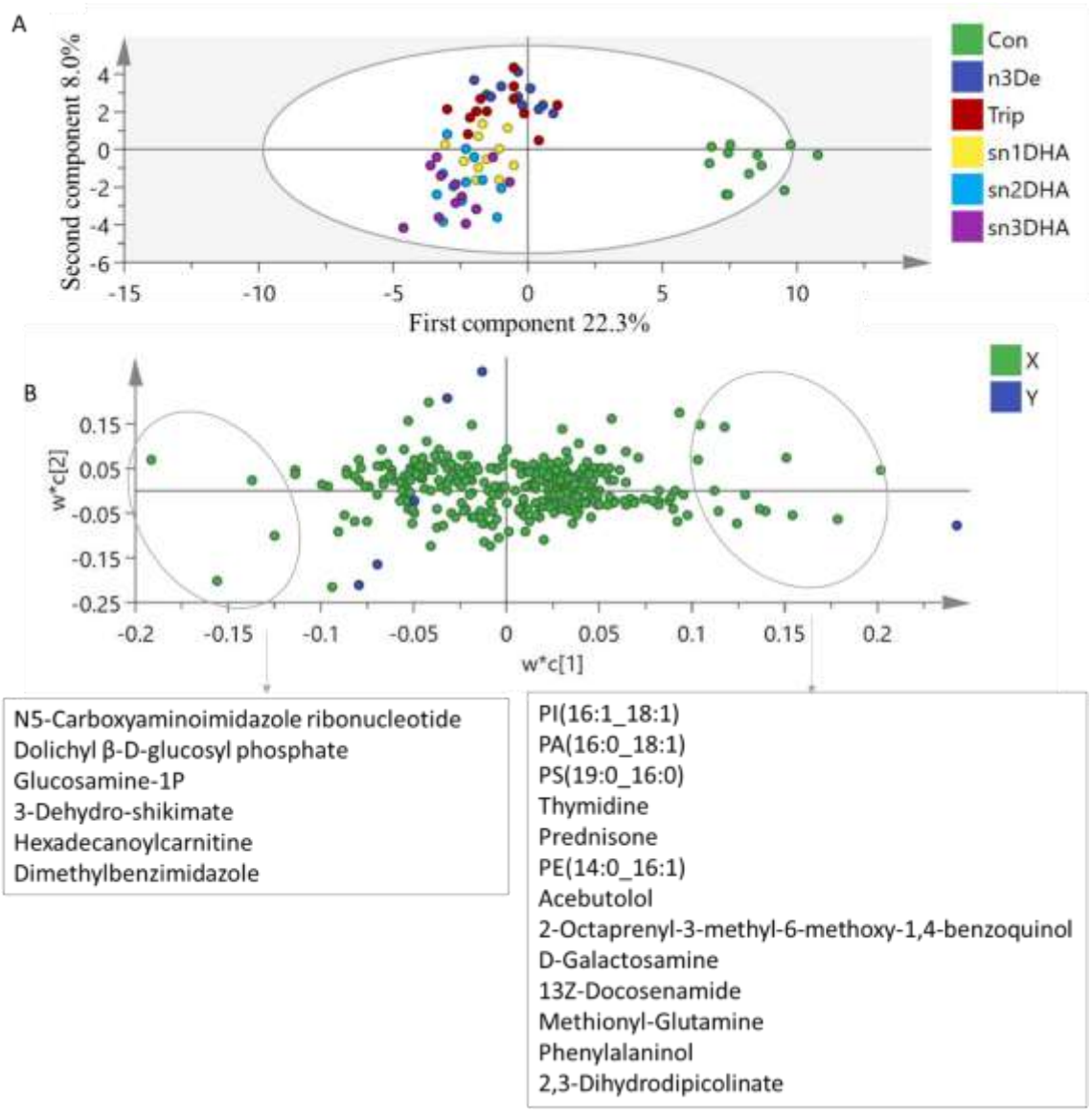

Figure S4. PLS-DA score plot (A) and loading plot (B) based on identified metabolites from all groups. Those metabolites in the right circle with positive w*c value (a value generated from combination of the X-weights, w*, and Y-weights, c) such as thymidine, 13Z-docosenamide, and 2,3-dihydrodipicolinate were higher in the Con group compared to the other groups. Those metabolites in the left circle with negative w*c value such as N5-carboxy aminoimidazole ribonucleotide, glucosamine-1P, and dimethylbenzimidazole were lower in the Con group compared to the other groups fed with n-3 fatty acid deficient peanut-oil-based rodent chow.

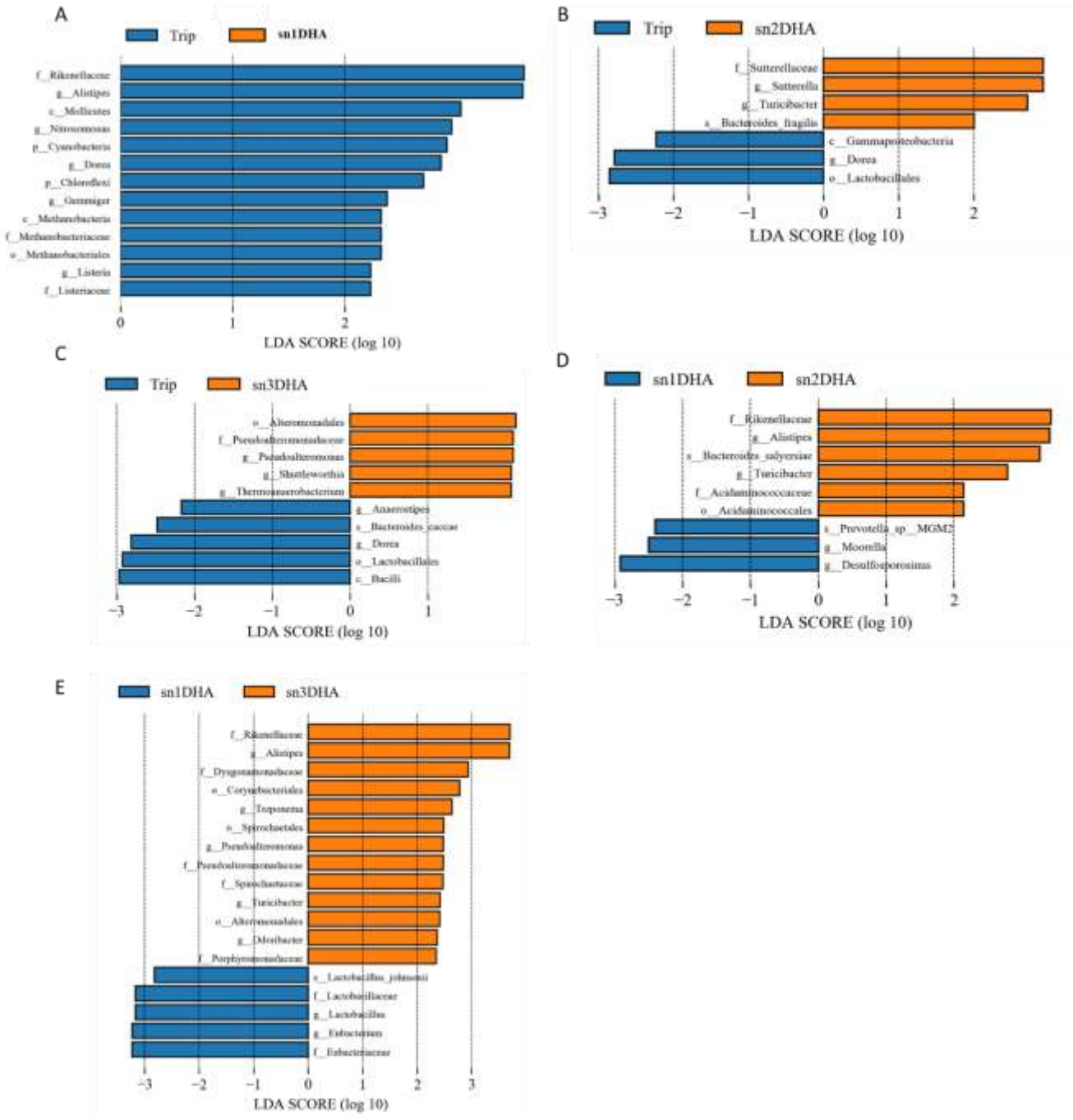

Figure S5. Significantly changed gut microbes revealed by LEfSe (LDA Effect Size).

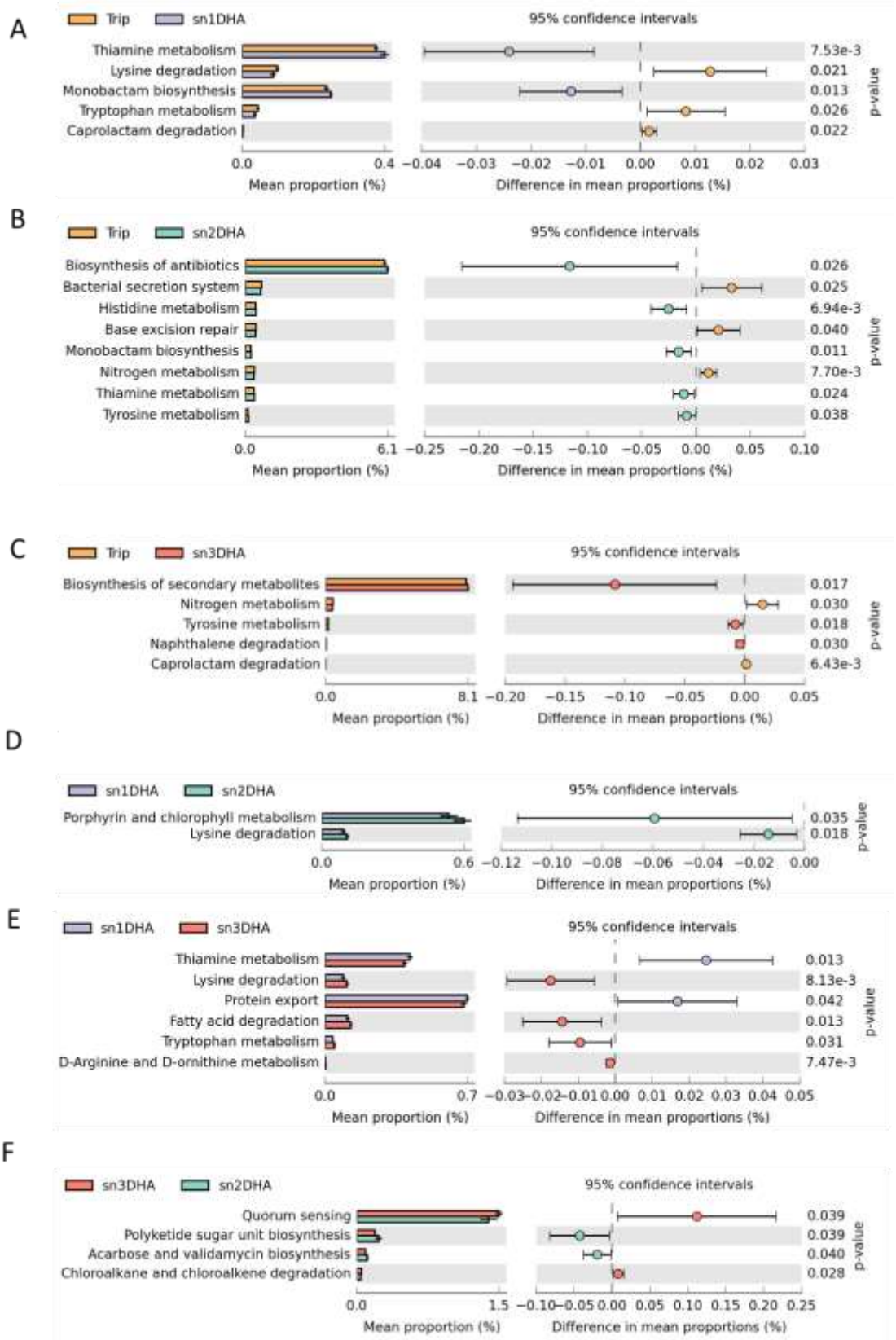

Figure S6. Extended error bar plot identifying significant altered KEGG pathway of gut microbiot